JCTC Journal of Chemical Theory and Computation

pubs.acs.org/JCTC Article

Reference Vertical Excitation Energies for Transition Metal Compounds

Denis Jacquemin,* Fábris Kossoski, Franck Gam, Martial Boggio-Pasqua,* and Pierre-François Loos*

Cite This: J. Chem. Theory Comput. 2023, 19, 8782−8800 Read Online

ABSTRACT: To enrich and enhance the diversity of the QUEST database of highly accurate excitation energies [Véril, M.; et al. *Wiley Interdiscip. Rev.: Comput. Mol. Sci.* **2021**, *11*, e1517], we report vertical transition energies in transition metal compounds. Eleven diatomic molecules with a singlet or doublet ground state containing a fourth-row transition metal (CuCl, CuF, CuH, ScF, ScH, ScO, ScS, TiN, ZnH, ZnO, and ZnS) are considered, and the corresponding excitation energies are computed using high-level coupled-cluster (CC) methods, namely, CC3, CCSDT, CC4, and CCSDTQ, as well as multiconfigurational methods such as CASPT2 and NEVPT2. In many cases, to provide more comprehensive benchmark data, we also provide full configuration interaction estimates computed with the configuration interaction using a perturbative selection made iteratively (CIPSI) method. Based on these calculations, theoretical best estimates of the transition energies are established in both the aug-cc-pVDZ and aug-cc-pVTZ basis sets. This allows us to accurately assess the performance of the CC and multiconfigurational methods for this specific set of challenging transitions. Furthermore, comparisons with experimental data and previous theoretical results are also reported.

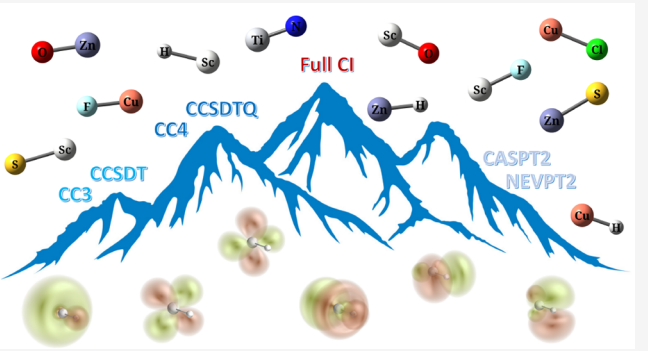

I. INTRODUCTION

Understanding the electronic structure of transition metal compounds[1] is critical for unraveling their specific behaviors and optimize their applications in a wide range of fields, such as chemistry and biology.[2] Their electronic structure is characterized by the presence of partially filled d orbitals in the transition metal atoms, which gives rise to their unique properties such as variable oxidation states,[3] magnetic behavior,[4−6] and catalytic activity.[7] The empty d orbitals can participate in chemical reactions,[8] allowing for the transfer of electrons during redox processes.[9] Transition metal catalysts find applications in various industrial processes, including hydrogenation, oxidation, and carbon−carbon bond formation.[10−12]

From a general perspective, investigating molecular excited states is essential for understanding their reactivity, photophysical properties, and catalytic behavior. Indeed, the presence of the excited electron modifies the electronic structure of the molecule, affecting reactions such as bond activation, insertion, or reductive processes.[13−17] The excited states of molecules containing transition metals have very peculiar characteristics and reactivity due to the presence of the transition metal atom. For example, in photocatalysis, the absorption of light can lead to the formation of reactive excited states that participate in photochemical reactions.[18]

Experimentally characterizing excited states in transition metal compounds is challenging due to their often short lifetimes and low transition probabilities. Transient absorption spectroscopy,[19] time-resolved techniques,[20] and advanced spectroscopic methods are required to observe and analyze the excited-state behavior. Additionally, the identification and assignment of the observed spectral features are challenging due to the complexity of the excited-state manifold in these systems.[21]

From a theoretical point of view, the study of excited states in transition metal compounds presents several challenges due to their complex electronic structures and intricate interactions.[21−28] First, they often require sophisticated theoretical methods to accurately describe the electronic structures of both their ground state and their excited states.[29−39] These calculations are computationally demanding and require the use of high-level quantum-chemical approaches,[40] such as multireference methods,[41] to account for the strong correlation effects present in many transition metal systems (see below).[42−55] Second, the large number of electrons and basis functions involved in these calculations further adds to the

Received: September 29, 2023
Revised: October 24, 2023
Accepted: October 27, 2023
Published: November 15, 2023

https://doi.org/10.1021/acs.jctc.3c01080
J. Chem. Theory Comput. 2023, 19, 8782−8800

computational complexity. Third, transition metal compounds often exhibit multiple spin states, which affects not only their reactivity but also their magnetic properties.[56] This leads to the accumulation of excited states with potentially the same spin and spatial symmetries in a very narrow energy window, which complicates the interpretation of experimental results and theoretical calculations.[39,57]

As mentioned above, transition metal derivatives often exhibit strong (or static) correlation, which refers to the intricate interactions among electrons occupying the d orbitals. Strong correlation is often a signature of the multiconfigurational character of the electronic wave function, meaning that the ground state and/or excited states cannot be accurately described by a single Slater determinant (single-reference wave function) but require a linear combination of determinants (multireference wave function) to accurately capture the electronic structure. The remaining dynamic correlation must also be taken into account, as it systematically plays a crucial role in describing the excited states.

To accurately describe the multiconfigurational character and strong electron correlation, methods based on configuration interaction (CI) are commonly employed.[58] This class of methods allows for mixing of different electronic configurations and provides a flexible framework to capture the electronic correlation effects. If one considers all possible electronic configurations, the resulting full CI (FCI) wave function corresponds to the exact solution of the Schrödinger equation within a given one-electron basis set. Unfortunately, the ensemble of these configurations, known as the Hilbert space, has a size that grows exponentially fast with system size, leading to a prohibitive computational cost in most applications.

Multiconfigurational self-consistent field methods, such as complete-active-space self-consistent field (CASSCF), account for all determinants generated by distributing a given number of electrons in a given number of active orbitals, therefore incorporating, by design, static correlation. Besides, unlike in CI, orbitals are variationally optimized. The missing dynamic correlation is usually recovered via low-order perturbation theory, as in complete-active-space second-order perturbation theory (CASPT2)[59−61] or *N*-electron valence state second-order perturbation theory (NEVPT2).[62−65] For CASSCF-based methods, selecting an appropriate active space is critical for capturing the important electron correlation effects while keeping the computational cost manageable. In transition metal compounds, the active space typically involves the d orbitals of the metal center and the orbitals involved in the metal−ligand interactions. Choosing an appropriate active space is a delicate balance between including a sufficient number of active orbitals to describe the correlation effects and keeping a reasonable computational cost.

Coupled-cluster (CC) methods offer an alternative approach, based on an exponential ansatz of the wave function, that allows for size-extensive and systematically improvable calculations toward the FCI limit. These methods exhibit polynomial scaling and have been extensively studied in the literature.[66−71] Coupled-cluster methods systematically incorporate higher levels of excitation to improve accuracy. For instance, CC with singles and doubles (CCSD),[72−76] CC with singles, doubles, and triples (CCSDT),[77−80] and CC with singles, doubles, triples, and quadruples (CCSDTQ)[81−85] can be obtained by successively adding higher excitation levels. The computational cost of these methods scales as $O(N^6)$, $O(N^8)$, and $O(N^{10})$, respectively. Moreover, to reduce computational expenses, each of these methods can be approximated by the CC*n* family of methods. This family includes CC2 ($O(N^5)$),[86,87] CC3 ($O(N^7)$),[88−92] and CC4 ($O(N^9)$).[93−97] These variants provide cost-effective alternatives while still maintaining acceptable levels of accuracy compared with their "complete" variant. Excited-state energies and properties can be obtained within the CI framework by searching for higher roots of the CI matrix and their corresponding eigenvectors. Similarly, at the CC level, one can access excited states using the equation of motion (EOM)[75,79,98−102] or linear response (LR)[74,100,103−105] formalisms.

II. THE QUEST DATABASE

Benchmark sets and their corresponding reference data serve as a cornerstone in electronic structure theory, supporting the development, validation, and improvement of computational methods for both the ground state[24,106−124] and the excited states.[125−141] In the context of molecular excited states, a benchmark set refers to a collection of molecules with known reference data that is used to evaluate the accuracy, reliability, and limitations of computational methods in predicting the properties of electronic excited states such as excitation energies, oscillator strengths, transition dipole moments, and other spectroscopic observables.

Benchmark sets provide a standardized framework for evaluating the performance of different computational methods in predicting excited-state properties, contributing to the reproducibility and transparency of computational studies in the field. By comparing different methods against each other, researchers can identify the strengths and weaknesses of different approaches and gain insights into their limitations, hence guiding the development of new computational methods for electronic excited states. Besides, these investigations also assist researchers and practitioners in selecting appropriate methods for specific applications and/or molecules.

The reference data are typically obtained from highly accurate theoretical calculations or experimental measurements. Their accuracy and reliability are mandatory for ensuring the meaningfulness of the benchmarking process. In some cases, reference data may be obtained from experiments, such as spectroscopic measurements or photochemical data, but these experimental values are not always available or may have large uncertainties.[142] The selection of molecules for a benchmark set aims to cover a diverse range of electronic structures and properties, including different types of excited states as well as a variety of chemical environments and molecular sizes. Importantly, the list should also include challenging cases that test the capabilities of the methods under investigation.

Since 2018, our research groups have made significant efforts to develop a comprehensive and diverse database of highly accurate vertical excitation energies for small- and medium-sized (organic) molecules. This database, named QUEST,[57,143] has been meticulously curated and expanded over time. It currently comprises seven subsets, as illustrated in Figure 1:

- QUEST#1: This subset consists of 110 vertical excitation energies (and oscillator strengths) in small molecules containing one to three non-hydrogen atoms.[144] Primarily focused on singly excited states, the theoretical

https://doi.org/10.1021/acs.jctc.3c01080
J. Chem. Theory Comput. 2023, 19, 8782−8800

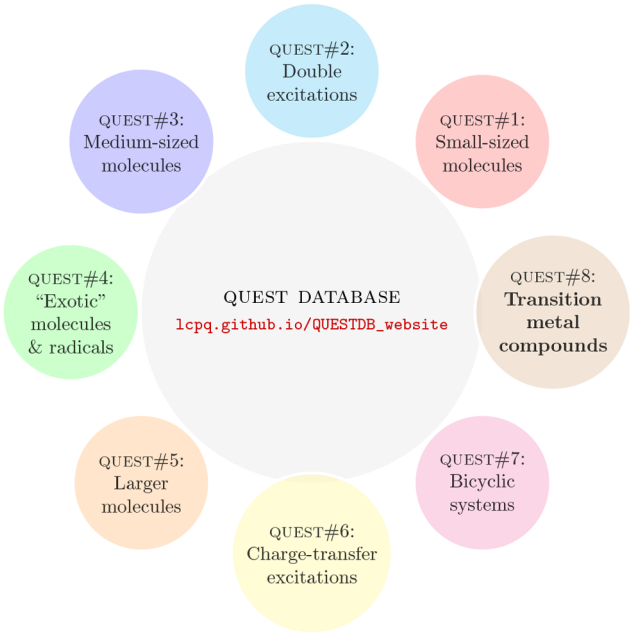

Figure 1. Eight subsets composing the QUEST database of highly accurate excitation energies with the inclusion of a new subset gathering excited states of transition metal compounds (QUEST#8).

best estimates (TBEs) were mainly determined using FCI calculations.

- QUEST#2: Comprising 20 vertical transition energies for doubly excited states in 14 small and medium-sized molecules,[145] this subset relied predominantly on FCI calculations to define the TBEs, except for the largest molecules in the set.
- QUEST#3: This subset encompasses 238 excitation energies (and oscillator strengths) for 27 medium-sized molecules containing four to six non-hydrogen atoms.[146] The TBEs in this subset were originally defined using CCSDT or CCSDTQ methods, and more recent improvements have been made with CC4 and CCSDTQ approaches.[147,148]
- QUEST#4: Composed of two distinct parts, this subset includes an "exotic" subset of 30 vertical excitation energies for closed-shell molecules containing F, Cl, P, and Si atoms and a "radical" subset of 51 doublet−doublet transitions in 24 small open-shell molecules.[149] In total, there are 81 TBEs, mostly obtained with FCI.
- QUEST#5: Featuring 80 excitation energies in 13 (mostly large) molecules, this subset mostly contains TBE calculations at the CCSDT level.[57]
- QUEST#6: Specifically designed for the study of intramolecular charge-transfer transitions, this subset provides highly accurate vertical excitation energies for 30 such transitions in 17 π-conjugated compounds obtained at the CCSDT level.[96]
- QUEST#7: This subset contains 91 vertical excitation energies for 10 bicyclic molecules computed at the CC3 or CCSDT levels.[150]

As evidenced by the above description, QUEST employs FCI and high-order CC methods to generate highly accurate reference data in triple-ζ basis sets, alongside additional basis set corrections when possible. In most cases, geometry optimization was carried out at the CC3/aug-cc-pVTZ level. A significant advantage of the QUEST dataset is its independence from experimental values, eliminating potential biases associated with experiments and facilitating direct theoretical comparisons. The employed protocol ensures uniformity, enabling straightforward cross-comparisons. This approach allowed the benchmarking of a wide range of excited-state wave function methods, including those accounting for double and triple excitations as well as multiconfigurational methods. Besides the QUEST database, chemically accurate theoretical 0−0 energies have been computed, providing a more direct comparison to experimental data.[142,151,152] Presently, our ongoing efforts are dedicated to obtaining highly accurate excited-state properties such as dipole moments and oscillator strengths for small and medium-sized molecules.[153−156]

The creation of the QUEST dataset involved a very significant computational effort, with numerous calculations performed for each of the associated articles.[57,96,144−146,149,150] To access and manipulate the data, a web application has been developed and hosted on a GitHub repository (https://github.com/LCPQ/QUESTDB_website). The web application can be accessed at https://lcpq.github.io/QUESTDB_website, providing users with the ability to plot statistical indicators for selected subsets of molecules, methods, and basis sets.

The utilization of the QUEST database as a benchmark for excited-state methods has gained attraction among research groups worldwide. For instance, the database has been employed to assess orbital-optimized DFT for double excitations,[157,158] multistate DFT,[159] and TD-DFT.[160] Additionally, it has facilitated the evaluation of hybrid[161] and double hybrid[162−165] functionals, quantum Monte Carlo methods for excited states,[166−170] multiconfiguration methods,[155,171−173] and others.[174−177] These studies demonstrate the widespread use of the QUEST database as a valuable resource for the rigorous assessment of excited-state methods.

In this study, we aim to enhance the diversity of our database and incorporate chemically challenging cases. Specifically, we perform excited-state calculations for 11 diatomic molecules with a singlet or doublet ground state, each containing a fourth-row transition metal: CuCl, CuF, CuH, ScF, ScH, ScO, ScS, TiN, ZnH, ZnO, and ZnS. To establish highly accurate reference vertical excitation energies, we determine TBEs using a combination of FCI and CCSDTQ data in the aug-cc-pVDZ and aug-cc-pVTZ basis sets. Leveraging these reference values, we conduct a comprehensive assessment of lower-order CC methods, namely, CC3, CCSDT, and CC4, as well as benchmark the performance of both CASPT2 and NEVPT2 for this set of excitations. This contributes to a more thorough understanding of the capabilities and limitations of these computational methods in addressing the electronic excitations of the aforementioned diatomic molecules.

Spin−orbit coupling, which arises from the relativistic effects on the electrons' motion, is important in transition metal compounds, as it couples the spin states of the electrons and affects the energy ordering and mixing of the excited states. Properly accounting for relativistic effects is crucial when performing experiment vs theory comparisons, and it requires specified theoretical approaches to accurately describe the electronic structure and energetics. Here, because our aim is to rely solely on theoretical values and to perform theory versus theory comparisons, we eschew taking into account relativistic effects. We refer the interested reader to ref 43 for a state-of-the-art treatment of these systems based on single- and

https://doi.org/10.1021/acs.jctc.3c01080
J. Chem. Theory Comput. 2023, 19, 8782−8800

multireference CC methodologies that incorporate core−valence and relativistic effects as well as complete basis set extrapolations.

III. COMPUTATIONAL METHODOLOGY

The ground-state geometries of the singlet and doublet states have been optimized in the frozen-core approximation at the CC3/aug-cc-pVTZ and UCCSD(T)/aug-cc-pVTZ levels of theory, respectively. These calculations were performed with CFOUR[178] and GAUSSIAN16,[179] respectively. Large frozen cores have been systematically selected. (Additional calculations for small cores can be found in the Supporting Information, showing that the deviations between small- and large-frozen-core excitation energies are small for the considered excited states.) The optimized bond lengths are reported in Table I

Table I. Electronic Ground-State Symmetry and Corresponding Bond Length (in Å) of the 11 Diatomic Molecules Considered Herein

		bond length (Å)	
system	electronic ground state	this work	expt[43]
ScH	$1\ ^1\Sigma^+$	1.796	1.7754
ScO	$1\ ^2\Sigma^+$	1.699	1.6661
ScF	$1\ ^1\Sigma^+$	1.788	1.787
ScS	$1\ ^2\Sigma^+$	2.168	2.1353
TiN	$1\ ^2\Sigma^+$	1.599	1.5802
CuH	$1\ ^1\Sigma^+$	1.480	1.4626
CuF	$1\ ^1\Sigma^+$	1.758	1.7449
CuCl	$1\ ^1\Sigma^+$	2.075	2.0512
ZnH	$1\ ^2\Sigma^+$	1.603	1.5935
ZnO	$1\ ^1\Sigma^+$	1.700	1.7047
ZnS	$1\ ^1\Sigma^+$	2.068	2.0464

alongside the electronic ground-state symmetry of each system and experimental values extracted from ref 43. For all of the systems considered, we performed calculations using two diffuse-containing Gaussian basis sets (aug-cc-pVDZ and aug-cc-pVTZ).

FCI vertical excitation energies were obtained with selected CI calculations[180−195] based on the configuration interaction using a perturbative selection made iteratively (CIPSI) algorithm.[196] All these calculations were performed with QUANTUM PACKAGE[197] following the same protocol as in our previous studies.[144−146] Extrapolation errors are estimated following the procedure of ref 57.

For the singlet excited states of closed-shell systems, the CC calculations were carried out using CFOUR,[178] which offers an efficient implementation of high-order CC methods up to quadruples.[95] For the triplet excited states of closed-shell derivatives, we relied on PSI4[198] for the (U-)CC3 calculations and MRCC[199] for the (U-)CCSDT and (U-)CCSDTQ calculations. For the open-shell transition metal derivatives, the latter two codes were used as well for the corresponding CC calculations, which were achieved starting from the restricted open-shell Hartree−Fock (ROHF) solution.

The multiconfigurational calculations were performed using a state-averaged (SA) CASSCF wave function, which included the ground state and at least the excited states of interest. Additional excited states were included in some cases to address convergence and root-flipping issues. The CASPT2 calculations were performed within the RS2 contraction scheme (unless otherwise stated), as implemented in MOLPRO,[200] with a default IPEA shift of $0.25E_h$.[201,202] To mitigate the intruder state problem, a level shift of $0.3E_h$ was systematically applied.[203,204] In some cases, we have also performed partially contracted (PC) NEVPT2 calculations as well as CASPT2 calculations without IPEA shift (labeled as NOIPEA). These additional data can be found in the Supporting Information, where one would also find strongly contracted (SC) NEVPT2 results. For each system and transition, the Supporting Information also provides a detailed description of the active spaces for each symmetry representation.

IV. RESULTS AND DISCUSSION

The results for the singlet and triplet transitions are reported in Table II, whereas those for the doublet transitions are reported in Table III. Table IV contains our TBEs, along with selected available results from the literature. To the best of our knowledge, these are usually the most up-to-date theoretical or experimental data for each state. The interested reader can consult the corresponding references to find more exhaustive comparisons with prior results, which is not our focus here. The convergence of the CC energies toward the TBEs is shown in Figure 2. We consider 22 out of our 67 TBEs to be unsafe (meaning errors potentially greater than 1 kcal/mol or 0.043 eV). Despite the uncertainties for this subset of TBEs, one can still gauge the convergence profile of the CC series, since a new TBE would only set a new reference energy.

It is important to bear in mind that in most cases our computed vertical excitation energies are not directly comparable to the previously reported data shown in Table IV. There are three reasons for that. First, ground-state geometries might be slightly different. Second, there are differences between the Hamiltonian employed in the calculations and the true physical Hamiltonian. Here we adopt the nonrelativistic Coulombic Hamiltonian, which neglects spin−orbit coupling and relativistic effects. These effects are important for transition metal compounds and would have been taken into account had the goal been to obtain a quantitative comparison with experimental observables. Ignoring them is justifiable, however, because we are interested in obtaining accurate nonrelativistic excitation energies, which are far greater in magnitude than the contribution from the above-mentioned effects. For this reason, when comparing the present results with previous calculations, we present those that similarly ignore relativistic effects, when available. A third aspect is that the excitation energies listed in Table IV often correspond to different observables. Experiments typically report specific vibronic transitions, particularly for those between vibrational ground states of electronic ground and excited states, the so-called 0−0 energies, also referred to as T_0. In turn, theoretical studies usually present potential energy curves from which the minimum-energy separation between ground and excited states (the adiabatic or T_e energy) is obtained. Modeling the vibrational levels would provide information about the 0−0 energy, which can be compared with experimental values.[136,137,139,140,142,151,152] Here, instead, we provide very accurate vertical excitation energies. Considering nonrelativistic potential energy curves, our vertical value represents an upper bound for T_e and would also be expected to be higher than the 0−0 value in most cases.

In the following, we discuss in detail each transition metal compound grouped into different families. When comparing

https://doi.org/10.1021/acs.jctc.3c01080
J. Chem. Theory Comput. 2023, 19, 8782−8800

Table II. Vertical Excitation Energies (in eV) of the Lowest Singlet and Triplet Excited States of ScH, ScF, CuH, CuF, CuCl, ZnO, and ZnS at Various Levels of Theory; 3, T, 4, Q, CAS, and NEV Stand for CC3, CCSDT, CC4, CCSDTQ, CASPT2(IPEA), and PC-NEVPT2, Respectively[a]

		aug-cc-pVDZ							aug-cc-pVTZ						
mol.	state	3	T	4	Q	CAS	NEV	FCI	3	T	4	Q	CAS	NEV	FCI
ScH	1 $^1\Delta$(4s,3d)	0.639	0.607	0.606	0.606	0.519	0.538	0.606(1)	0.698	0.672	0.671	0.672	0.515	0.535	0.671(1)
	1 $^1\Pi$(4s,3d)	0.837	0.818	0.819	0.820	0.783	0.786	0.820(1)	0.890	0.874	0.875	0.875	0.764	0.769	0.875(1)
	2 $^1\Sigma^+$(4s,3d)	1.894	1.846	1.839	1.836	2.060	2.003	1.836(1)	1.900	1.856	1.848	1.845	2.040	1.983	
	2 $^1\Pi$(4s^2,3d^2)	2.300	2.197	2.185	2.181	2.122	2.141	2.181(1)	2.331	2.233	2.219	2.215	2.129	2.149	
	1 $^3\Delta$(4s,3d)	0.365	0.361		0.364	0.278	0.292	0.363(1)	0.445	0.443		0.446	0.280	0.295	0.445(1)
	1 $^3\Pi$(4s,3d)	0.573	0.563		0.565	0.520	0.532	0.565(1)	0.625	0.618		0.621	0.510	0.523	0.620(1)
	1 $^3\Sigma^+$(4s,3d)	0.807	0.818		0.820	0.821	0.834	0.820(1)	0.840	0.850		0.852	0.813	0.827	0.851(1)
	2 $^3\Pi$(4s,3d)	1.870	1.835		1.832	1.845	1.832		1.852	1.820		1.817	1.853	1.839	
ScF	1 $^1\Delta$(4s,3d)	0.823	0.759	0.816	0.787	0.559	0.612	0.797(1)	0.925	0.863	0.919	0.890	0.554	0.584	0.903(4)
	1 $^1\Pi$(4s,3d)	1.602	1.550	1.579	1.564	1.353	1.406	1.574(3)	1.698	1.648	1.676	1.661	1.344	1.409	1.653(26)
	2 $^1\Sigma^+$(4s,3d)	2.382	2.351	2.351	2.346	2.378	2.385	2.356(18)	2.437	2.410	2.408	2.404	2.366	2.382	
	2 $^1\Pi$(4s^2,3d^2)	2.806	2.756	2.777	2.758	2.479	2.562		2.884	2.840	2.854	2.837	2.478	2.569	
	1 $^3\Delta$(4s,3d)	0.550	0.490		0.519	0.292	0.341	0.528(2)	0.665	0.606			0.292	0.318	0.647(3)
	1 $^3\Pi$(4s,3d)	1.053	1.017		1.032	0.896	0.923	1.037(4)	1.122	1.089			0.896	0.933	
	1 $^3\Sigma^+$(4s,3d)	1.414	1.394		1.401	1.389	1.403		1.471	1.452			1.389	1.408	
	2 $^3\Pi$(4s^2,3d^2)	2.625	2.469		2.469	2.409	2.478		2.664	2.593			2.422	2.503	
CuH	2 $^1\Sigma^+$(3d,4s)	3.101	2.905	3.205	3.009	3.102		3.051(4)	3.120	2.928	3.222	3.031	3.143		3.080(7)
	1 $^1\Delta$(3d,4s)	3.701	3.554	4.082	3.718	3.558			3.743	3.593	4.110	3.754	3.614		
	1 $^1\Pi$(3d,4s)	3.651	3.537	4.072	3.707	3.571		3.788(26)	3.700	3.580	4.102	3.746	3.623		3.829(28)
	2 $^1\Pi$(3d,4s)	5.527	5.379	5.664	5.470	5.408			5.557	5.410	5.686	5.497	5.449		
	3 $^1\Sigma^+$(3d,4p)	5.560	5.639	5.888	5.713	5.971			5.618	5.682	5.922	5.751	6.038		
	1 $^3\Sigma^+$(3d,4s)	2.600	2.411		2.493	2.536		2.514(5)	2.626	2.439			2.572		2.539(37)
	1 $^3\Pi$(3d,4s)	3.456	3.280		3.453	3.333		3.522(11)	3.508	3.327			3.393		3.561(37)
	1 $^3\Delta$(3d,4s)	3.591	3.393		3.561	3.422			3.631	3.432			3.479		
	2 $^3\Pi$(3d,4s)	4.865	4.678		4.762	4.691			4.900	4.716			4.746		
CuF	2 $^1\Sigma^+$(3d,4s)	2.571	2.391	2.723	2.508	2.528		2.561(10)	2.596	2.416	2.744		2.539		2.604(28)
	1 $^1\Pi$(3d,4s)	2.623	2.518	2.934	2.660	2.632		2.751(8)	2.671	2.560	2.970		2.674		
	1 $^1\Delta$(3d,4s)	3.209	3.077	3.500	3.211	3.014		3.285(49)	3.245	3.111	3.528		3.045		
	2 $^1\Pi$(3d,4s)	5.681	5.870	5.966	5.914	6.028			5.752	5.919	6.011		6.047		
	1 $^3\Sigma^+$(3d,4s)	2.121	1.882		1.992	1.941		2.017(20)	2.158	1.918			1.987		2.066(58)
	1 $^3\Pi$(3d,4s)	2.390	2.211		2.355	2.317		2.421(28)	2.439	2.258			2.367		
	1 $^3\Delta$(3d,4s)	3.001	2.799		2.937	2.758			3.037	2.838			2.793		
	2 $^3\Pi$(3d,4s)	5.679	5.715		5.766	5.791			5.760	5.767			5.825		
CuCl	2 $^1\Sigma^+$(σ,4s)	3.072	2.880	3.227	3.004	3.088	3.333		3.090	2.898	3.242		3.149	3.030	
	1 $^1\Pi$(3d,4s)	3.001	2.880	3.235	3.008	2.965	2.971		3.044	2.912	3.263		3.049	3.015	
	1 $^1\Delta$(3d,4s)	3.562	3.392	3.843	3.540	3.533	3.539		3.596	3.422	3.874		3.472	3.454	
	1 $^3\Sigma^+$(σ,4s)	2.681	2.460			2.626	2.529		2.708	2.486			2.692	2.578	
	1 $^3\Pi$(3d,4s)	2.770	2.591			2.661	2.654		2.811	2.631			2.845	2.818	
	1 $^3\Delta$(3d,4s)	3.364	3.145			3.281	3.277		3.398	3.179			3.229	3.203	
ZnO	1 $^1\Pi$(2p,4s)	0.812	0.732	0.771	0.759	0.523	0.556	0.771(2)	0.835	0.760	0.791		0.530	0.557	
	2 $^1\Sigma^+$(σ,4s)	3.244	3.450	3.394	3.415	3.767	3.720	3.417(22)	3.260	3.466	3.400		3.763	3.718	

https://doi.org/10.1021/acs.jctc.3c01080
J. Chem. Theory Comput. 2023, 19, 8782−8800

Table II. continued

mol.	state	aug-cc-pVDZ							aug-cc-pVTZ						
		3	T	4	Q	CAS	NEV	FCI	3	T	4	Q	CAS	NEV	FCI
	$1\ ^1\Delta(2p,4p)$	4.300	4.548	4.671	4.611	4.365	4.399		4.352	4.602	4.705		4.381	4.413	
	$1\ ^1\Sigma^-(2p,4p)$	4.354	4.592	4.718	4.660	4.691	4.591		4.401	4.638	4.746		4.692	4.587	
	$1\ ^3\Pi(2p,4s)$	0.542	0.445			0.314	0.347	0.506(13)	0.574	0.481			0.332	0.358	
	$1\ ^3\Sigma^+(\sigma,4s)$	1.884	1.731			1.590	1.578	1.793(16)	1.880	1.729			1.570	1.554	
ZnS	$1\ ^1\Pi(3p,4s)$	0.769	0.755	0.778	0.774	0.735	0.701	0.816(3)	0.802	0.787	0.801		0.774	0.724	0.814(14)
	$2\ ^1\Sigma^+(\sigma,4s)$	3.626	3.616	3.630	3.622	3.974	3.911	3.673(51)	3.651	3.642	3.649		3.978	3.915	3.867(116)
	$1\ ^1\Delta(3p,4p)$	4.181	4.162	4.213	4.200	4.198	4.191		4.225	4.204	4.242		4.231	4.216	
	$1\ ^1\Sigma^-(3p,4p)$	4.225	4.213	4.279	4.267	4.315	4.252		4.252	4.238	4.294		4.335	4.258	
	$1\ ^3\Pi(3p,4s)$	0.520	0.503			0.528	0.496		0.565	0.546			0.573	0.524	
	$1\ ^3\Sigma^+(\sigma,4s)$	2.343	2.302			2.311	2.304		2.351	2.306			2.314	2.306	

[a]The CASPT2 values for CuF are performed in the R2C formalism.

the available data with those of our TBEs, we always refer to the aug-cc-pVTZ values. Next, we present the global view of our full set of results, discussing the performance of the different methodologies for transition metal diatomics and comparing them with previous subsets of the QUEST database devoted to organic compounds.[57]

A. ScH and ScF. Out of the 11 transition metal diatomics considered here, the excitation energies of ScH present the fastest convergence along the CC series. Already at the CC3 level, most energies lie within the desired chemical accuracy window (±1 kcal/mol or 0.043 eV), as shown in Figure 2. The largest difference (0.12 eV) appears for the fourth singlet state, $2\ ^1\Pi(4s^2,3d^2)$, which is acceptable since this state has significant doubly excited character, making CC3 less efficient. The accuracy is significantly improved at the CCSDT level and beyond. These outcomes are unsurprising, as only four electrons are correlated in our (large) frozen core approximation for ScH. Hence, CCSDTQ is equivalent to FCI. In CASPT2 and NEVPT2, all active electrons are correlated, though within a subset of orbitals, and the computed excitation energies deviate more from the TBEs than CC3. There is an average increase of 0.04 eV in the TBEs of ScH on going from aug-cc-pVDZ to aug-cc-pVTZ. It is worth mentioning that the $1\ ^3\Delta(4s,3d)$ state of ScH has the lowest TBE of the QUEST database, of only 0.364 eV for the aug-cc-pVDZ basis set and 0.446 eV for the aug-cc-pVTZ basis set.

Our vertical TBEs are compatible with the 0−0 experimental energies,[205] the former being higher by 0.13 to 0.21 eV. The TBEs are also close to the T_e energies calculated at the multireference configuration interaction (MRCI) level,[206] appearing higher in energy by 0.06 to 0.22 eV. The only exception concerns the $2\ ^3\Pi(4s,3d)$ state, whose TBE is lower-lying by −0.03 eV, possibly due to the occurrence of an avoided crossing with a higher-lying $3\ ^3\Pi$ state.[206]

Moving to ScF, we first note that both the $2\ ^1\Pi(4s^2,3d^2)$ and $2\ ^3\Pi(4s^2,3d^2)$ excited states are doubly excited with respect to the ground state. Although the number of active electrons jumps from four to 10, the convergence along the CC series remains quite fast, although not on par with the ScH case. CC3 nevertheless delivers chemically accurate excitation energies for most states, except for the $2\ ^3\Pi(4s^2,3d^2)$ state, whose energy is more overestimated than the others. In fact, third-order methods like CC3 and CCSDT produce fairly accurate excitation energies for the two doubly excited states, with the largest difference between the TBEs produced with CC3 and the aug-cc-pVDZ basis set for the triplet state (0.156 eV). This is somewhat surprising given the typically poorer performance of these methods in describing such excited states.[145] Ramping up to CCSDTQ produces excitation energies too low by only 0.01 eV for the states whose TBEs are obtained with CIPSI. Considering the complete set of 11 transition metals investigated here, we find the TBEs to be somewhat larger with the aug-cc-pVTZ basis set, by 0.04 eV on average and up to 0.08 eV. Taking into account the safe TBEs only, ScF shows the most pronounced basis set effects from our set, with the largest increase in the TBEs of 0.124 eV for the $2\ ^3\Pi(4s^2,3d^2)$ state, followed by 0.119 eV for the $1\ ^3\Delta(4s,3d)$ state.

The TBEs of ScF can be correlated with the experimental T_e and 0−0 energies[211,212] as well as with the T_e values calculated with MRCI plus Davidson correction (MRCI+Q).[213] However, the overall largest discrepancies from the current set of transition metal diatomics are seen for this system. Compared to experiment, the TBEs can be lower by 0.12 eV [2

https://doi.org/10.1021/acs.jctc.3c01080
J. Chem. Theory Comput. 2023, 19, 8782−8800

Table III. Vertical Excitation Energies (in eV) of the Lowest Doublet Excited States of ScO, ScS, TiN, and ZnH at Various Levels of Theory; 3, T, 4, Q, CAS, and NEV Stand for CC3, CCSDT, CC4, CCSDTQ, CASPT2(IPEA), and PC-NEVPT2, Respectively

		aug-cc-pVDZ						aug-cc-pVTZ					
mol.	state	3	T	Q	CAS	NEV	FCI	3	T	Q	CAS	NEV	FCI
ScO	1 $^2\Pi$(4s,3d)	2.000	2.029	2.029	2.032	2.036	2.032(1)	1.998	2.028	2.028	2.037	2.040	2.037(3)
	1 $^2\Delta$(4s,3d)	2.248	2.023	2.084	1.824	1.829	2.107(1)	2.270	2.052	2.109	1.794	1.797	2.133(3)
	2 $^2\Sigma^+$(4s,3d)	2.484	2.584	2.564	2.575	2.594	2.563(6)	2.482	2.584	2.564	2.569	2.591	2.572(19)
	2 $^2\Pi$(2p,4s)	3.502	3.467	3.550	3.590	3.489		3.534	3.506	3.570	3.632	3.502	
ScS	1 $^2\Delta$(4s,3d)	1.376	1.185	1.262	0.981	0.974	1.300(2)	1.405	1.231	1.299	0.936	0.934	1.340(8)
	1 $^2\Pi$(4s,3d)	1.579	1.450	1.485	1.495	1.466	1.495(8)	1.574	1.459	1.491	1.476	1.434	1.512(4)
	2 $^2\Sigma^+$(4s,3d)	1.663	1.572	1.591	1.637	1.590	1.590(1)	1.653	1.571	1.589	1.634	1.574	1.593(5)
	2 $^2\Pi$(3p,4s)	2.161	2.021	2.070	2.134	2.140		2.185	2.063	2.093	2.215	2.338	
TiN	1 $^2\Delta$(4s,3d)	1.330	0.869	0.970	0.884	0.916	1.027(1)	1.386	0.916		0.840	0.874	1.066(5)
	2 $^2\Delta$(σ,3d)	1.796	1.965	1.969	2.241	2.242	2.008(6)	1.863	2.000		2.227	2.222	
	1 $^2\Pi$(4s,3d)	1.979	2.023	2.009	2.045	2.030		1.976	2.008		2.027	2.014	
ZnH	1 $^2\Pi$(4s,4p)	2.862	2.834	2.839	2.843		2.851(4)	2.874	2.846		2.862		2.882(17)
	2 $^2\Sigma^+$(σ,4s)	4.474	4.452	4.448	4.483		4.456(13)	4.499	4.478		4.510		4.483(43)
	3 $^2\Sigma^+$(4s,5s)	5.070	5.027	5.035	5.062		5.045(3)	5.097	5.056		5.097		5.115(5)
	4 $^2\Sigma^+$(4s,5p)	5.674	5.628	5.635	5.582		5.644(7)	5.691	5.647		5.598		5.689(21)
	2 $^2\Pi$(4s,5p)	6.118	6.069	6.076	6.062		6.081(8)	6.147	6.100		6.106		6.126(12)

$^1\Sigma^+$(4s,3d)] or higher by 0.49 eV [1 $^1\Pi$(4s,3d)]. This hints at a more significant vibrational relaxation in the excited states than in ScH.

B. CuH, CuF, and CuCl. CuH has 12 active electrons, whereas the halogen-containing compounds CuF and CuCl have 18 in the present (large) frozen core calculations. For some excited states of CuH and CuF, safe TBEs of FCI quality could be attained. For others (and for CuCl), we rely on CCSDTQ or CASPT2 as the TBEs, which are therefore considered unsafe. These systems present strong oscillations in the CC series, having the overall slowest convergence from our set of transition metal compounds. In many cases, detailed below, even CCSDTQ is unable to produce values within the chemically accurate window that stem from FCI calculations. The unfavorable convergence profile is independent of the atom bonded to Cu, which is the culprit for the observed behavior. The $4s^1$ unpaired electron is strongly coupled to the $3d^{10}$ shell, making correlation effects very pronounced in Cu-containing systems. This contrasts to the Zn atom, where the additional electron fills the $4s^2$ shell, such that a mean-field approximation is a much more suitable starting point than for the strongly correlated Cu atom.

For some states of CuH, the CIPSI calculations yield a small error bar and therefore directly provide trustworthy TBEs. Accounting for these states only, the average absolute errors are smaller with CCSDTQ (0.05 eV) than with CASPT2 (0.12 eV), besides being more systematic with the former method. We thus expect CCSDTQ to perform similarly better than CASPT2 for the other excited states, where FCI is unattainable, and for this reason, CCSDTQ is the method of choice for obtaining their TBEs. Given the systematic underestimation of CCSDTQ with respect to the available FCI estimates, by 0.02 to 0.08 eV with the aug-cc-pVDZ basis set, the true TBEs are probably greater (by a comparable amount) than those obtained with CCSDTQ. The same reasoning holds for CuF. The average error for the five states where FCI/aug-cc-pVDZ estimates are accessible is smaller for CCSDTQ (0.06 eV) than for CASPT2 (0.12 eV), the former method underestimating the TBEs by 0.02 to 0.09 eV. The CCSDTQ results for the remaining three excited states thus provide our TBEs, which are in turn expected to be a bit too low. When only CCSDT results are available (which is the case for the triplet states of CuCl), we rely on CASPT2 for the TBEs, based on the same argument. Despite the missing FCI estimates for CuCl, the similarity between its excited states and those of CuH and CuF makes us believe that CCSDTQ would also be more accurate than CASPT2 for this system. However, we note that the CC error formally increases more rapidly with the number of electrons than the CASPT2 one. Enlarging the basis set from aug-cc-pVDZ to aug-cc-pVTZ affects all TBEs of CuH quite similarly, which increase by 0.03 to 0.06 eV, averaging at 0.04 eV. For CuF, they increase by 0.01 to 0.05 eV, with an average of 0.03 eV.

For the three Cu-containing compounds, the profiles of the CC convergence are similar for most states. CC3 provides fairly decent excitation energies (typically within 0.2 eV of the TBEs), considering its relatively low computational cost. CCSDT often becomes less accurate and underestimates the TBEs, which are then overestimated by CC4. Overall, CC3 is more accurate (and cheaper) than the higher-order CCSDT and CC4 models. CCSDTQ is probably enough to achieve an accuracy of 0.1 eV. To ensure chemical accuracy (0.043 eV), at least pentuple excitations should likely be accounted for in CC models.

The three species present overall very large discrepancies between CC4 and CCSDTQ and between CC3 and CCSDT, from 0.2 to 0.3 eV. This is considerably more than usually observed for typical excited states of organic species.[144,147−149] They also show the overall largest differences between the TBEs and the various CC models. For instance, the 1 $^1\Pi$(3d,4s) state of CuH is one of the most challenging of our set. With the aug-cc-pVDZ basis set, the TBE of 3.788 eV obtained with FCI is considered safe. This TBE presents the largest difference to CCSDT (3.537 eV), of −0.251 eV, and to CC4 (4.072 eV), of +0.284 eV, and the second largest difference to CCSDTQ (3.707 eV), of −0.081 eV. For the aug-cc-pVTZ basis set, the same state also presents the largest energy difference obtained with CCSDTQ (3.746 eV) and the safe TBE from FCI (3.829 eV), of −0.083 eV.

https://doi.org/10.1021/acs.jctc.3c01080
J. Chem. Theory Comput. 2023, 19, 8782−8800

Table IV. TBEs (in eV) in the aug-cc-pVDZ (AVDZ) and aug-cc-pVTZ (AVTZ) Basis Sets for the 11 Diatomic Molecules and the Corresponding Composite Methods to Generate Them

		aug-cc-pVDZ		aug-cc-pVTZ		literature	
mol.	state	TBE	method	TBE	method	expt	theor
ScH	1 $^1\Delta$(4s,3d)	0.606	CCSDTQ	0.672	CCSDTQ	0.519[b]	0.509[c]
	1 $^1\Pi$(4s,3d)	0.820	CCSDTQ	0.875	CCSDTQ	0.670[b]	0.710[c]
	2 $^1\Sigma^+$(4s,3d)	1.836	CCSDTQ	1.845	CCSDTQ	1.683[b]	1.703[c]
	2 $^1\Pi$(4s^2,3d^2)	2.181	CCSDTQ	2.215	CCSDTQ	2.089[b]	2.151[c]
	1 $^3\Delta$(4s,3d)	0.364	CCSDTQ	0.446	CCSDTQ		0.225[c]
	1 $^3\Pi$(4s,3d)	0.565	CCSDTQ	0.621	CCSDTQ		0.430[c]
	1 $^3\Sigma^+$(4s,3d)	0.820	CCSDTQ	0.851	CCSDTQ		0.728[c]
	2 $^3\Pi$(4s,3d)	1.832	CCSDTQ	1.817	CCSDTQ		1.852[c]
ScO	1 $^2\Pi$(4s,3d)	2.032	FCI	2.037	FCI	2.057[d]	2.070(6)[e]
	1 $^2\Delta$(4s,3d)	2.107	FCI	2.133	FCI	1.915[d]	1.950(5)[e]
	2 $^2\Sigma^+$(4s,3d)	2.563	FCI	2.572	FCI	2.559[f]	
	2 $^2\Pi$(2p,4s)	3.550[a]	CCSDTQ	3.570[a]	CCSDTQ		
ScF	1 $^1\Delta$(4s,3d)	0.797	FCI	0.903	FCI	0.568[g]	0.478[j]
	1 $^1\Pi$(4s,3d)	1.574	FCI	1.671	FCI/AVDZ + CCSDTQ/AVTZ − CCSDTQ/AVDZ	1.184[g]	1.107[j]
	2 $^1\Sigma^+$(4s,3d)	2.346	CCSDTQ	2.404	CCSDTQ	2.527[g]	2.004[j]
	2 $^1\Pi$(4s^2,3d^2)	2.758	CCSDTQ	2.837	CCSDTQ	2.750[g]	2.521[j]
	1 $^3\Delta$(4s,3d)	0.528	FCI	0.647	FCI	0.242[h]	0.215[j]
	1 $^3\Pi$(4s,3d)	1.037	FCI	1.109	FCI/AVDZ + CCSDT/AVTZ − CCSDT/AVDZ	0.774[i]	0.719[j]
	1 $^3\Sigma^+$(4s,3d)	1.401	CCSDTQ	1.459	CCSDTQ/AVDZ + CCSDT/AVTZ − CCSDT/AVDZ		1.073[j]
	2 $^3\Pi$(4s^2,3d^2)	2.469	CCSDTQ	2.593	CCSDTQ/AVDZ + CCSDT/AVTZ − CCSDT/AVDZ		2.347[j]
ScS	1 $^2\Delta$(4s,3d)	1.300	FCI	1.340	FCI		1.003[k]
	1 $^2\Pi$(4s,3d)	1.495	FCI	1.512	FCI	1.375[l]	1.418[k]
	2 $^2\Sigma^+$(4s,3d)	1.590	FCI	1.593	FCI	1.544[l]	1.493[k]
	2 $^2\Pi$(3p,4s)	2.070[a]	CCSDTQ	2.093[a]	CCSDTQ		
TiN	1 $^2\Delta$(4s,3d)	1.027	FCI	1.066	FCI	0.934[m]	0.946[n]
	2 $^2\Delta$(σ,3d)	2.008	FCI	2.043	FCI/AVDZ + CCSDT/AVTZ − CCSDT/AVDZ		
	1 $^2\Pi$(4s,3d)	2.009	CCSDTQ	1.994	CCSDTQ/AVDZ + CCSDT/AVTZ − CCSDT/AVDZ	2.013[m]	2.01[n]
CuH	2 $^1\Sigma^+$(3d,4s)	3.051	FCI	3.080	FCI	2.905[o]	3.009[p]
	1 $^1\Delta$(3d,4s)	3.718[a]	CCSDTQ	3.754[a]	CCSDTQ	3.530[o]	
	1 $^1\Pi$(3d,4s)	3.788	FCI	3.829	FCI	3.381[o]	3.406[p]
	2 $^1\Pi$(3d,4s)	5.470[a]	CCSDTQ	5.497[a]	CCSDTQ	5.542[o]	6.035[p]
	3 $^1\Sigma^+$(3d,4p)	5.713[a]	CCSDTQ	5.751[a]	CCSDTQ		3.349[p]
	1 $^3\Sigma^+$(3d,4s)	2.514	FCI	2.550	FCI/AVDZ + CASPT2/AVTZ − CASPT2/AVDZ	2.418[q]	2.604[p]
	1 $^3\Pi$(3d,4s)	3.522	FCI	3.582	FCI/AVDZ + CASPT2/AVTZ − CASPT2/AVDZ	3.276[o]	3.159[p]
	1 $^3\Delta$(3d,4s)	3.561[a]	CCSDTQ	3.618[a]	CCSDTQ/AVDZ + CASPT2/AVTZ − CASPT2/AVDZ	3.492[o]	
	2 $^3\Pi$(3d,4s)	4.762[a]	CCSDTQ	4.817[a]	CCSDTQ/AVDZ + CASPT2/AVTZ − CASPT2/AVDZ		5.209[p]
CuF	2 $^1\Sigma^+$(3d,4s)	2.561	FCI	2.572	FCI/AVDZ + CASPT2/AVTZ − CASPT2/AVDZ	2.445[r]	2.31[s]
	1 $^1\Pi$(3d,4s)	2.751	FCI	2.793	FCI/AVDZ + CASPT2/AVTZ − CASPT2/AVDZ	2.512[r]	2.41[s]
	1 $^1\Delta$(3d,4s)	3.285[a]	FCI	3.316[a]	FCI/AVDZ + CASPT2/AVTZ − CASPT2/AVDZ		2.93[s]
	2 $^1\Pi$(3d,4s)	5.914[a]	CCSDTQ	5.933[a]	CCSDTQ/AVDZ + CASPT2/AVTZ − CASPT2/AVDZ		
	1 $^3\Sigma^+$(3d,4s)	2.017	FCI	2.063	FCI/AVDZ + CASPT2/AVTZ − CASPT2/AVDZ	1.808[r]	1.81[t]
	1 $^3\Pi$(3d,4s)	2.421	FCI	2.471	FCI/AVDZ + CASPT2/AVTZ − CASPT2/AVDZ	2.177[r]	2.17[t]
	1 $^3\Delta$(3d,4s)	2.937[a]	CCSDTQ	2.972[a]	CCSDTQ/AVDZ + CASPT2/AVTZ − CASPT2/AVDZ	2.827[r]	2.65[t]
	2 $^3\Pi$(3d,4s)	5.766[a]	CCSDTQ	5.800[a]	CCSDTQ/AVDZ + CASPT2/AVTZ − CASPT2/AVDZ		
CuCl	2 $^1\Sigma^+$(σ,4s)	3.004[a]	CCSDTQ	3.065[a]	CCSDTQ/AVDZ + CASPT2/AVTZ − CASPT2/AVDZ	2.848[u]	2.75[s]
	1 $^1\Pi$(3d,4s)	3.008[a]	CCSDTQ	3.092[a]	CCSDTQ/AVDZ + CASPT2/AVTZ − CASPT2/AVDZ	2.861[u]	2.78[s]
	1 $^1\Delta$(3d,4s)	3.540[a]	CCSDTQ	3.479[a]	CCSDTQ/AVDZ + CASPT2/AVTZ − CASPT2/AVDZ		3.20[s]
	1 $^3\Sigma^+$(σ,4s)	2.626[a]	CASPT2	2.692[a]	CASPT2	2.352[u]	2.43[t]
	1 $^3\Pi$(3d,4s)	2.661[a]	CASPT2	2.845[a]	CASPT2	2.540[u]	2.62[t]
	1 $^3\Delta$(3d,4s)	3.281[a]	CASPT2	3.229[a]	CASPT2	3.134[u]	3.00[t]
ZnH	1 $^2\Pi$(4s,4p)	2.851	FCI	2.882	FCI	2.90[v]	2.93[w]
	2 $^2\Sigma^+$(σ,4s)	4.456	FCI	4.482	FCI/AVDZ + CCSDT/AVTZ − CCSDT/AVDZ	3.42[v]	4.54[w]
	3 $^2\Sigma^+$(4s,5s)	5.045	FCI	5.115	FCI	5.09[v]	5.04[w]
	4 $^2\Sigma^+$(4s,5p)	5.644	FCI	5.663	FCI/AVDZ + CCSDT/AVTZ − CCSDT/AVDZ		5.70[w]
	2 $^2\Pi$(4s,5p)	6.081	FCI	6.126	FCI		6.09[w]
ZnO	1 $^1\Pi$(2p,4s)	0.771	FCI	0.791	FCI/AVDZ + CC4/AVTZ − CC4/AVDZ	0.615[x]	0.54[y]
	2 $^1\Sigma^+$(σ,4s)	3.417	FCI	3.423	FCI/AVDZ + CC4/AVTZ − CC4/AVDZ		3.75[y]
	1 $^1\Delta$(2p,4p)	4.611[a]	CCSDTQ	4.645[a]	CCSDTQ/AVDZ + CC4/AVTZ − CC4/AVDZ		4.90[y]

https://doi.org/10.1021/acs.jctc.3c01080
J. Chem. Theory Comput. 2023, 19, 8782−8800

Table IV. continued

		aug-cc-pVDZ		aug-cc-pVTZ		literature	
mol.	state	TBE	method	TBE	method	expt	theor
	$1\ ^1\Sigma^-(2p,4p)$	4.660[a]	CCSDTQ	4.688[a]	CCSDTQ/AVDZ + CC4/AVTZ − CC4/AVDZ		4.76[y]
	$1\ ^3\Pi(2p,4s)$	0.506	FCI	0.542	FCI/AVDZ + CCSDT/AVTZ − CCSDT/AVDZ	0.305[x]	0.29[y]
	$1\ ^3\Sigma^+(\sigma,4s)$	1.793	FCI	1.791	FCI/AVDZ + CCSDT/AVTZ − CCSDT/AVDZ	1.875[z]	2.03[y]
ZnS	$1\ ^1\Pi(3p,4s)$	0.816	FCI	0.814	FCI		0.682[aa]
	$2\ ^1\Sigma^+(\sigma,4s)$	3.622[a]	CCSDTQ	3.641[a]	CCSDTQ/AVDZ + CC4/AVTZ − CC4/AVDZ		3.718[aa]
	$1\ ^1\Delta(3p,4p)$	4.200	CCSDTQ	4.229	CCSDTQ/AVDZ + CC4/AVTZ − CC4/AVDZ		4.279[aa]
	$1\ ^1\Sigma^-(3p,4p)$	4.267	CCSDTQ	4.282	CCSDTQ/AVDZ + CC4/AVTZ − CC4/AVDZ		4.239[aa]
	$1\ ^3\Pi(3p,4s)$	0.503[a]	CCSDT	0.546[a]	CCSDT		0.456[aa]
	$1\ ^3\Sigma^+(\sigma,4s)$	2.302[a]	CCSDT	2.306[a]	CCSDT		2.266[aa]

[a]Unsafe TBE, which means that the error is possibly greater than 0.043 eV. [b]0−0 energy from emission spectroscopy of ref 205. [c]T_e energy from MRCI calculations of ref 206. [d]Vertical energy obtained from the T_e chemiluminescence spectroscopy of refs 207 and 208 corrected by the vibrational term, as explained in ref 209 and averaged over the two spin−orbit components. [e]Vertical energy (and statistical uncertainty) from FCIQMC calculations of ref 209. [f]T_e energy from ref 210. [g]T_e energy from emission spectroscopy of ref 211. [h]T_e energy from emission spectroscopy of ref 212. [i]0−0 energy from emission spectroscopy of ref 212. [j]T_e energy from MRCI+Q calculations of ref 213. [k]T_e energy from MRCI+Q calculations of ref 214. [l]0−0 energy from emission spectroscopy of ref 215. [m]T_e energy from emission spectroscopy of ref 216. [n]T_e energy from MRCI calculations of ref 217. [o]T_e experimental energy from ref 210. [p]T_e energy from MRCI+Q+DKH calculations of ref 218. [q]0−0 energy from photoelectron spectroscopy of ref 219. [r]T_e energy from absorption spectroscopy of ref 220. [s]T_e energy from EOM-CCSD calculations of ref 221. [t]T_e energy from CCSD(T) calculations of ref 221. [u]0−0 energy from fluorescence spectroscopy of ref 222. [v]0−0 experimental energy from ref 210. [w]Vertical energy from MS-CASPT2 calculations of ref 53. [x]0−0 energy from photoelectron spectroscopy of ref 223. [y]0−0 energy from MRCI+Q calculations of ref 224. [z]0−0 energy from photoelectron spectroscopy of ref 225. [aa]0−0 energy from MRCI+Q calculations of ref 226.

Despite these difficulties in the convergence of the CC series, there is an overall good agreement among our TBEs and the previous results for CuH, CuF, and CuCl. Starting with CuH, our TBEs appear at −0.04 to 0.45 eV relative to the T_e experimental energies[210] [0−0 energy in the case of the $1\ ^3\Sigma^+(3d,4s)$ state[219]]. They are also consistent with MRCI+Q calculations (with relativistic effects), except for the $3\ ^1\Sigma^+(3d,4p)$ state, which is much higher in energy in all our calculations (TBE of 5.751 eV with the larger basis set) than in the previous one (3.349 eV).[218] This state has also been assigned as $3\ ^1\Sigma^+$ in ref 218, so the reason for this discrepancy remains unclear.

The four states of CuF for which safe TBEs can be compared with experiment[220] appear higher in energy than the experimentally obtained T_e values from 0.13 to 0.29 eV. They are also consistent with previous CCSD(T) and EOM-CCSD calculations.[221] Our TBEs for the $1\ ^3\Delta(3d,4s)$ state are both close to and in between the experimental[220] and EOM-CCSD results.[221] For the $2\ ^1\Pi(3d,4s)$ and $2\ ^3\Pi(3d,4s)$ excited states, there are, to our knowledge, no previous data to compare our results with.

Our TBEs for CuCl are also consistent with the 0−0 experimental values,[222] which are overestimated by 0.09 to 0.34 eV. There is also a correspondence between our TBEs and the T_e values obtained from CCSD(T) calculations for the three triplet states[221] and from EOM-CCSD calculations for the three singlet states,[221] though with quite larger differences in general, from 0.23 to 0.40 eV.

C. ZnO and ZnS. ZnO and ZnS have 18 active electrons in our large frozen core approximation, the largest number in our set of transition metal diatomics (along with CuF and CuCl). Despite that, the convergence along the CC series can be considered satisfactory, being far superior to the case of Cu-containing compounds.

The CC estimates for both the $1\ ^1\Pi(2p,4s)$ and $1\ ^3\Pi(2p,4s)$ excited states of ZnO always fall within the chemically accurate region, even with CC3. Meanwhile, at least CCSDT is needed to reach the same level of accuracy for the $2\ ^1\Sigma^+(\sigma,4s)$ state, whereas the $1\ ^1\Delta(2p,4p)$ and $1\ ^1\Sigma^-(2p,4p)$ states are even more challenging and would require at least CCSDTQ, which provides our (unsafe) TBEs. For the latter two excited states, CC3 produces excitation energies largely underestimated by ca. 0.3 eV. CCSDT significantly reduces the errors, bringing the energies from 0.05 to 0.07 eV below their TBEs. However, CC4 does not lead to further improvement, as it overestimates the TBEs by around the same amount, 0.06 eV. CCSDTQ is taken as the TBE, but it is not clear whether this level of theory is enough to achieve chemical accuracy for these two excited states.

Our TBEs for ZnO are consistent with the previous reports on the 0−0 energies.[223−225] For the lowest singlet [$1\ ^3\Pi(2p,4s)$] and triplet [$1\ ^3\Pi(2p,4s)$] excited states, they exceed the experimental values[223,225] by 0.18 and 0.24 eV, respectively, and MRCI+Q calculations[224] by 0.25 eV (both states). These differences can be explained by the potential energy curves reported in ref 224, which indicate considerably stretched equilibrium geometries for these two excited states (more so for the $1\ ^3\Pi(2p,4s)$ state). Conversely, our TBE for the $1\ ^3\Sigma^+(\sigma,4s)$ state is smaller than the experimental energy and the MRCI+Q 0−0 energy by 0.08 and 0.24 eV, respectively. Here the ground- and excited-state bond distances are actually similar, and the underestimated TBE probably indicates that the excited-state zero-point vibrational energy is greater than the ground-state one.[224] There are no experimental data for the three higher-lying states, though our TBEs are systematically lower (by 0.07 to 0.33 eV) than the previous MRCI+Q values.[224]

For ZnS, CC3 can provide excitation energies with virtual chemical accuracy. It is rather surprising that it performs significantly better than for ZnO, considering that these two systems share the same excited-state character and number of active electrons. The $2\ ^1\Sigma^+(\sigma,4s)$ state is very well described already at the CC3 level, and the energy computed at higher-order CC levels fluctuates around the TBE (corresponding to the CCSDTQ value for this state). Despite the proximity between the CCSDTQ and FCI results, the residual statistical

https://doi.org/10.1021/acs.jctc.3c01080
J. Chem. Theory Comput. 2023, 19, 8782−8800

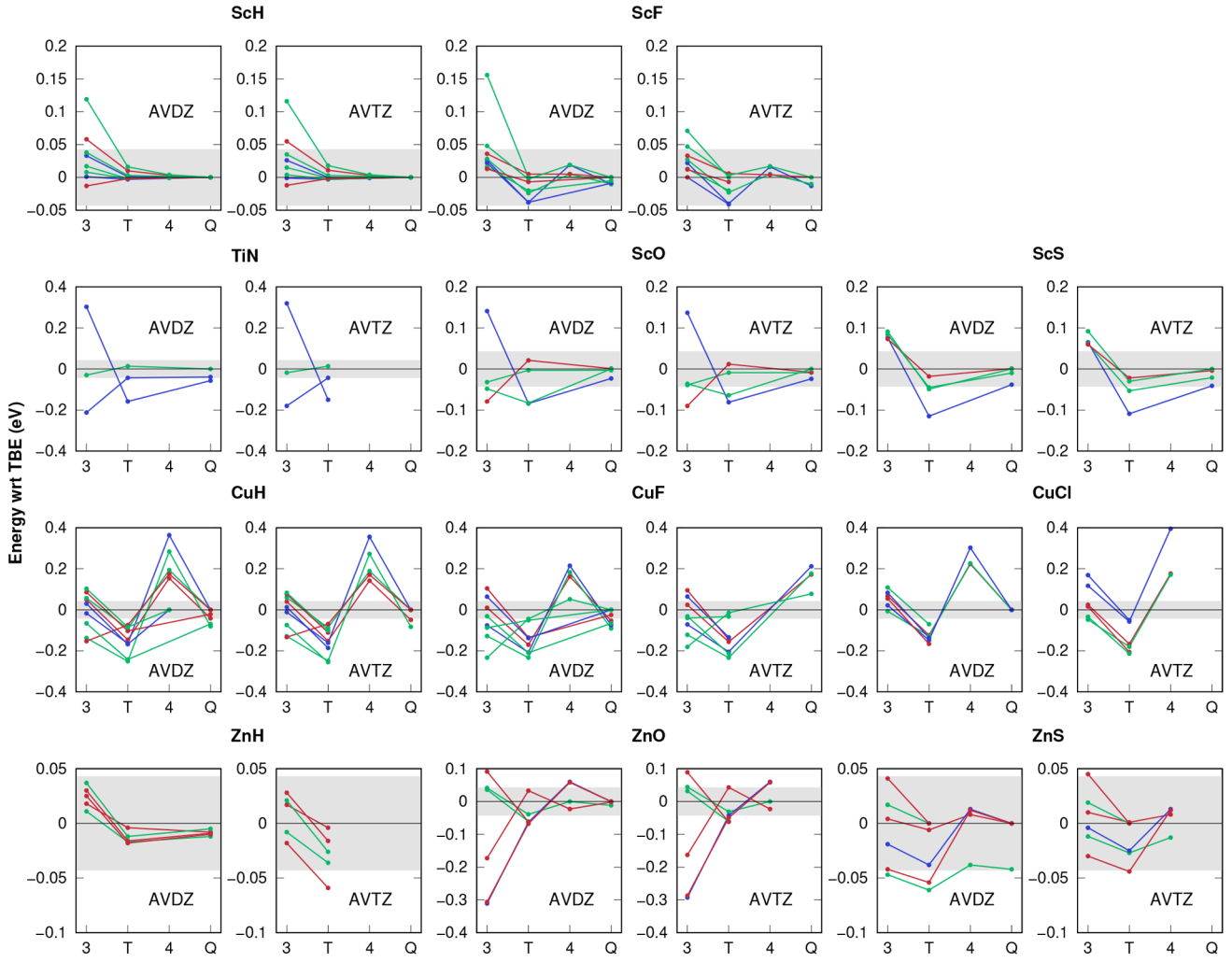

Figure 2. Convergence of the errors in excitation energies (with respect to the TBEs) along the coupled-cluster models (CC3, CCSDT, CC4, and CCSDTQ, denoted by their last digit in the figure), with the aug-cc-pVDZ (AVDZ) and aug-cc-pVTZ (AVTZ) basis sets, for Σ (red), Π (green), and Δ (blue) excited states of transition metal diatomics. The gray-shaded regions indicate deviations of ±0.043 eV with respect to the TBE.

uncertainty of the latter prevents us from claiming this TBE to be safe. For the two triplet excited states, 1 $^3\Pi(3p,4s)$ and 1 $^3\Sigma^+(\sigma,4s)$, CCSDT represents our TBEs, which are also considered unsafe. CCSDT slightly but systematically decreases the excitation energies of all states, which worsens the comparison with the TBEs for the 1 $^1\Pi(3p,4s)$, 1 $^1\Delta(3p,4p)$, and 1 $^1\Sigma^-(3p,4p)$ states. For the latter two, one needs CC4 to obtain a significant reduction in the errors.

The behavior of the first singlet excited state of ZnS, 1 $^1\Pi(3p,4s)$, stands out. Along the CC series (CC3, CCSDT, CC4, and CCSDTQ), its aug-cc-pVDZ excitation energy oscillates between 0.755 and 0.778 eV, a narrow interval of 0.023 eV. However, the apparent convergence can be ruled out with our FCI estimate of 0.816 eV, which represents our TBE. This value lies 0.042 eV above the CCSDTQ result and is significantly greater than the 0.003 eV statistical uncertainty of the FCI result. A similar trend is observed for the aug-cc-pVTZ basis set, although with a substantially smaller gap (0.013 eV) between FCI and CC4 (CCSDTQ is beyond computational reach). The convergence profile of the CC series is overall similar for both basis sets, somewhat less so than observed for ZnO. The TBEs of both ZnO and ZnS are slightly larger with the aug-cc-pVTZ basis set, by 0.02 eV in average.

Our computed TBEs for ZnS are once again close to previous MRCI+Q results for the 0−0 energies,[226] with differences between −0.08 to 0.13 eV, and the TBEs appear lower in energy for two of the six excited states, 2 $^1\Sigma^+(\sigma,4s)$ and 1 $^1\Delta(3p,4p)$. To the best of our knowledge, ZnS is the single compound investigated here for which there are no experimental excited-state data.

D. ScO and ScS. Both ScO and ScS are radicals having nine active electrons in our calculations. For most states, the CC series quickly converges to the TBEs, although less quickly than in the closed-shell ScH and ScF derivatives. In particular, the CC series is overall faster for ScF than for ScO. This reflects the impact of the additional electron from the F atom (compared with the O atom). The effect is small, however, compared to the case where the single electron difference is associated with the transition metals, as shown earlier for CuH and ZnH.

The 1 $^2\Delta(4s,3d)$ excited states of both ScO and ScS are the most challenging for these systems. CC3 and CCSDT display deviations of around 0.1 eV with respect to the TBE, by either overestimating or underestimating it, respectively. The

https://doi.org/10.1021/acs.jctc.3c01080
J. Chem. Theory Comput. 2023, 19, 8782−8800

description of these excited states becomes chemically accurate only at the CCSDTQ level. For both species, the CC convergence profile is quite insensitive to the basis set.

Our TBE for the 1 $^2\Pi$(4s,3d) state of ScO (2.037 eV) very closely matches both the vertical excitation energy obtained with accurate FCI quantum Monte Carlo (FCIQMC) calculations (2.070 eV)[209] and the estimated experimental vertical energy (2.057 eV), based on the T_e of refs 207 and 208 corrected for vibrational effects according to ref 209. In turn, the differences are greater for the 1 $^2\Delta$(4s,3d) state, with our TBE of 2.133 eV appearing higher in energy than both the FCIQMC one (1.950 eV)[209] and the estimated experimental vertical energy (1.915 eV).[207−209] Our TBEs place the 1 $^2\Delta$(4s,3d) state higher in energy than the 1 $^2\Pi$(4s,3d) state, in contrast to the available experimental and theoretical results. This is not too serious, however, as their energy gap is small, probably around 0.1 eV. For the 2 $^2\Sigma^+$(4s,3d) state, our TBE differs from the experimental T_e value[210] by 0.013 eV only. There are no previous data for the higher-lying 2 $^2\Pi$(2p,4s) excited state as far as we know.

The TBEs for the 1 $^2\Pi$(4s,3d) and 2 $^2\Sigma^+$(4s,3d) excited states of ScS are consistent with both the available 0−0 experimental values[215] and MRCI+Q T_e calculations,[214] being higher in energy by 0.05 to 0.14 eV. Whereas the lowest-lying excited state of ScS, 1 $^2\Delta$(4s,3d), remains to be observed experimentally, our TBE is higher than its MRCI+Q counterpart[214] by 0.34 eV, a larger difference than for the two higher-lying excited states. At least to some extent, this can be explained by the larger equilibrium bond distance of the first excited state, based on the MRCI+Q potential energy curves.[214]

E. TiN and ZnH. TiN and ZnH are radical species having nine and 13 active electrons in our calculations, respectively. The first excited state of TiN, 1 $^2\Delta$(4s,3d), shows slow convergence along the CC series. Compared to the TBE, its excitation energy is significantly overestimated at the CC3 level (0.30 to 0.32 eV, depending on the basis set), becoming underestimated at the CCSDT level (0.15 to 0.16 eV). The error further decreases with CCSDTQ, though not enough to reach chemical accuracy, as the computed energy appears 0.06 eV below the TBE with the aug-cc-pVDZ basis set. For the next state, 2 $^2\Delta$(σ,3d), CC3 also starts off with a large error, this time undeshooting the TBE by 0.18 to 0.21 eV. With the aug-cc-pVDZ basis set, the excitation energy obtained with CCSDT (1.965 eV) and CCSDTQ (1.969 eV) varies by only 0.004 eV, suggesting fairly converged results. However, the TBE of 2.008 eV (obtained with FCI) still lies 0.039 eV above the CCSDTQ energy. For both the 1 $^2\Delta$(4s,3d) and 2 $^2\Delta$(σ,3d) states of TiN, excitations beyond quadruples seem needed to reach chemical accuracy. The higher-lying excited state, 1 $^2\Pi$(4s,3d), displays a very small error already at the CC3 level, which becomes tinier at the higher CC levels. We further notice that the convergence profile up to CCSDT is quite insensitive to the choice of basis sets.

The TBEs for TiN are very close to the available T_e energies obtained experimentally[216] and with MRCI calculations.[217] Compared to the previously reported values, the TBE for the 1 $^2\Delta$(4s,3d) state is larger by 0.12 to 0.13 eV, whereas for the 1 $^2\Pi$(4s,3d) state, it is smaller by 0.07 eV. The 2 $^2\Delta$(σ,3d) excited state, although lying very close in energy to the 1 $^2\Pi$(4s,3d) state, has not been considered in the previous experimental and theoretical studies.

ZnH presents one of the most favorable CC convergence profiles with the aug-cc-pVDZ basis set. CC3 produces chemically accurate excitation energies with a slight overestimation. CCSDT is very accurate with the aug-cc-pVDZ basis set (within 0.02 eV of the TBEs) but slightly less accurate with the aug-cc-pVTZ basis set (with deviations up to 0.06 eV). That is a sizable basis set effect not seen in the other transition metal diatomics. CCSDTQ underestimates the TBEs by 0.005 to 0.015 eV only.

There is very good agreement between the TBEs of ZnH and the vertical excitation energies computed with multistate CASPT2 (MS-CASPT2) calculations,[53] with average absolute deviations of 0.06 eV for the five excited states considered here. Our CASPT2 results are even more accurate, with average absolute deviations of 0.03 eV. The TBEs are also very close to the available experimental data[210] for the 1 $^2\Pi$(4s,4p) and 3 $^2\Sigma^+$(4s,5s) 0−0 energies, underestimated and overestimated by only 0.02 eV, respectively. A much larger deviation of 1.06 eV is seen for the 2 $^2\Sigma^+$(σ,4s) state, probably reflecting its more stretched equilibrium bond distance.[53,210,227]

F. Global Statistics. We computed the mean signed error (MSE), mean absolute error (MAE), and root-mean-square error (RMSE), gathered in Table V, for both the CC and multiconfigurational methods considered here. They were evaluated with respect to the TBEs displayed in Table IV, including results for both basis sets and excluding the unsafe excited states (having errors potentially greater than 0.043 eV). Figure 3 shows the corresponding distribution of errors in the excitation energies. We collect the results from both basis sets because the main trends discussed in the following are rather insensitive to the choice of the basis set. The individual results for each one can be found in the Supporting Information.

Table V. Mean Signed Error (MSE), Mean Absolute Error (MAE), and Root-Mean-Square Error (RMSE) (in eV) with Respect to the TBEs for All of the States Assigned as Safe in Table IV

method	#	MSE	MAE	RMSE
CC3	90	+0.02	0.06	0.09
CCSDT	90	−0.05	0.06	0.09
CC4	34	+0.05	0.05	0.10
CCSDTQ	63	−0.02	0.02	0.03
CASPT2 (IPEA)	90	−0.08	0.12	0.16
CASPT2 (no IPEA)	90	−0.11	0.13	0.17
PC-NEVPT2	64	−0.08	0.12	0.16
SC-NEVPT2	64	−0.07	0.14	0.18

CC3 displays a fairly normal distribution of errors centered around zero (MSE of +0.02 eV), and the associated MAE is 0.06 eV only. By fully accounting for the triple excitations, CCSDT produces a negatively skewed distribution, with the MSE moving further away from zero (−0.05 eV) and the MAE remaining at 0.06 eV. Moving to CC4 only slightly reduces the MAE to 0.05 eV, whereas the underlying distribution becomes positively skewed with an MSE of +0.05 eV. CCSDTQ significantly reduces the errors with an MAE of only 0.02 eV and a somewhat negatively skewed distribution with an MSE of −0.02 eV. These very small errors would be expected, given that one-third of our safe TBEs stem from CCSDTQ calculations. Excluding these TBEs slightly shifts the MAE to 0.03 eV and the MSE to −0.03 eV.

https://doi.org/10.1021/acs.jctc.3c01080
J. Chem. Theory Comput. 2023, 19, 8782−8800

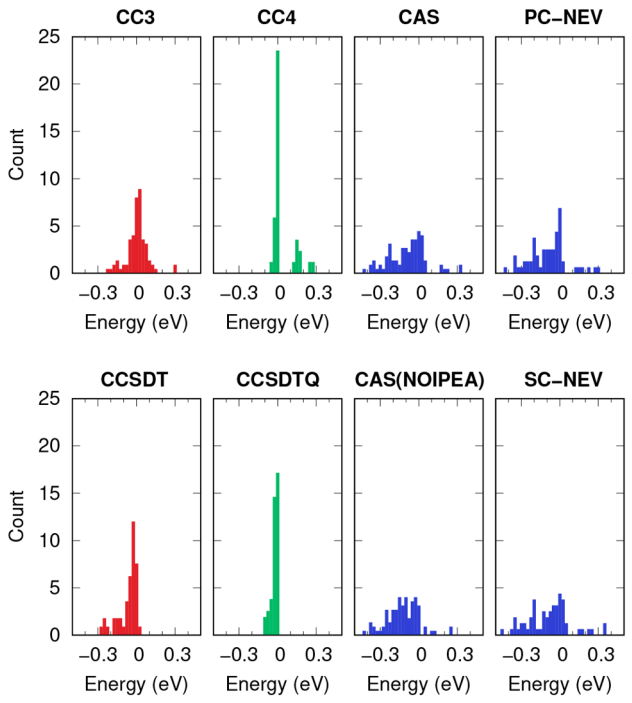

Figure 3. Distribution of the errors in excitation energies with respect to the safe TBEs of Table IV, with corresponding statistical errors presented in Table V. CAS and NEV stand for CASPT2 and NEVPT2, respectively.

In turn, the four different multiconfigurational approaches globally yield less accurate excitation energies than the CC models. The errors are quite comparable among them, with MAEs lying between 0.12 to 0.14 eV, MSEs of −0.11 and −0.08 eV, and negatively skewed distributions of the errors for all methods. CASPT2 with the IPEA shift is the most accurate out of the four, yet by a small margin. The effect of the IPEA shift is rather small, decreasing the MAE by 0.01 eV and making the MSE less negative by 0.03 eV. Similarly, the errors of PC-NEVPT2 and SC-NEVPT2 differ by no more than 0.02 eV. The comparable statistics obtained with the multiconfigurational methods endorse the choice of active spaces.

The accuracy of the tested CC models is overall independent of the basis set and comparable for singlets, doublets, and triplets. They are also similar across the different spatial symmetries, except for CC3, which performs better for Σ and Π (MAE of 0.05 eV) than for Δ (MAE of 0.09 eV) excited states. In contrast, the multiconfigurational methods display more pronounced differences, improving toward states of lower angular momentum. CASPT2/PC-NEVPT2 show MAEs of 0.21 eV/0.20 eV for Δ states, decreasing to 0.12 eV/0.10 eV for Π states and 0.08 eV/0.09 eV for Σ states. The multiconfigurational methods also deliver somewhat more accurate results for triplet than for singlet excited states, with respective MAEs of 0.12 and 0.15 eV according to CASPT2 and 0.11 and 0.14 eV based on PC-NEVPT2. Finally, the results are closer to those of the TBEs with the smaller basis set. Both CASPT2 and PC-NEVPT2 have an MAE of 0.11 eV with the aug-cc-pVDZ basis set, which slightly increases to 0.14 eV with the larger aug-cc-pVTZ basis set. The same trends concerning basis sets and spatial/spin symmetries are observed with or without the IPEA shift and for both PC-NEVPT2 and SC-NEVPT2.

It is interesting to compare the statistical errors for the present transition metal compounds with those for organic molecules obtained in the previous sets of the QUEST database. For the transition metals, CC3 offers an MAE of 0.06 eV. Although acceptable for most purposes, this error is greater than those previously found for other types of excited states. By comparing with previous QUEST subsets for which CCSDTQ or FCI TBEs are available, we find that the MAEs of CC3 become progressively smaller for the radicals of QUEST#4[149] (0.05 to 0.06 eV), the small molecules of QUEST#1[144] (0.03 eV), and the exotic molecules of QUEST#4[149] (0.01 eV). Even though CC3 performs very well in absolute terms, the MAEs for each type of transition span a range of 0.01 to 0.06 eV, which is large in relative terms. The accuracy is excellent for typical transitions of organic molecules, though less so for radicals and for transitions whose states present pronounced multiconfigurational character, such as the transition metal derivatives surveyed here.

A similar comparison of CASPT2 and NEVPT2 revealed a different picture. For the transition metal diatomics, the MAE of 0.12 to 0.14 eV is virtually the same as obtained for the medium-sized organic molecules of QUEST#3[146] with NEVPT2 (0.13 eV). Even though these results certainly depend on the choice of active space, they highlight the versatility of the CASPT2 and NEVPT2 methods in handling excited states with varying multiconfigurational characters while providing very similar levels of accuracy. This contrasts with the case of CC3, whose accuracy is more dependent on the type of transition. However, even for the challenging transitions in transition metal diatomics, the single-reference CC3 still outperforms the multiconfigurational alternatives. Interestingly, the IPEA shift has apparently a smaller impact on the transition metal diatomics than on organic systems.[155,171] In addition, the CASPT2 and NEVPT2 excitation energies are generally very similar for the systems considered here. Again, these observations further support our active spaces choices.

V. CONCLUSION

We have presented highly accurate vertical excitation energies for 67 excited states of 11 transition metal diatomic molecules comprising four different fourth-row elements (Sc, Ti, Cu, and Zn). To this end, we employed state-of-the-art excited-state methods, including selected CI, high-order equation-of-motion CC (CC3, CCSDT, CC4, and CCSDTQ), and multiconfigurational (CASPT2 and NEVPT2) methods. These calculations allowed us to provide nonrelativistic theoretical best estimates (based on the aug-cc-pVDZ and aug-cc-pVTZ basis sets) for the excitation energies of 67 states, 45 of which should be chemically accurate (errors less than 0.043 eV or 1 kcal/mol). These TBEs were compared with previous experimental and theoretical results. This contribution establishes the eighth subset of the QUEST database, the first comprising transition metals.

The convergence of the CC series toward TBE shows a pronounced dependence on the system. It is quite favorable for the Sc-containing species ScH, ScF, ScO, and ScS (somewhat less so for the latter two open-shell radicals), followed by the Zn-containing species ZnH, ZnO, and ZnS, although ZnO presents a few challenging excited states. TiN presents a slower convergence profile, whereas the Cu-containing compounds CuH, CuF, and CuCl proved to be the most challenging systems from the present set. This trend can be rationalized based on the occupancy of the 3d and 4s shells of the

https://doi.org/10.1021/acs.jctc.3c01080
J. Chem. Theory Comput. 2023, 19, 8782−8800

transition atom. Moving one position toward the center of the periodic table (from Sc to Ti and from Zn to Cu) increases the half-filled character of the shells, making the electronic correlation problem harder to tackle.

Despite the challenging multiconfigurational character of many excited states, CC3 performs surprisingly well, with an MAE of 0.06 eV, which is not significantly more than observed for transitions of small organic systems (0.01 to 0.06 eV). The higher-order CCSDT and CC4 levels produce comparable MAEs, and their corresponding error distributions are negatively and positively skewed, respectively. A further reduction in the errors only comes at the CCSDTQ level, with an MAE of 0.02 eV. In turn, the multiconfigurational methods are less accurate than CC3, with MAEs of 0.12 to 0.14 eV. However, we found quite consistent results with both forms of NEVPT2 and CASPT2 and a small effect introduced by the IPEA shift. Overall, if an accuracy of around 0.1 to 0.2 eV is acceptable, CC3 would be recommended. Otherwise, CCSDTQ is needed to achieve chemical accuracy, although it is still insufficient for the most difficult cases.

While the current reference vertical energies offer significant value, it is important to note that they do not take into account relativistic effects.[228] Incorporating such effects, which can significantly affect vertical transition energies in some cases, would be both a logical and formidable undertaking that holds substantial potential value for the electronic structure community.

■ ASSOCIATED CONTENT

Supporting Information

The Supporting Information is available free of charge at https://pubs.acs.org/doi/10.1021/acs.jctc.3c01080.

Comparison between small and large frozen-core calculations, additional CASSCF, CASPT2 (with and without IPEA shift), and (partially and strongly contracted) NEVPT2 data, and the detailed description and specification of the active space for each molecule and each transition (PDF)

Data calculated using different software packages, methods, and basis sets (XLSX)

Additional statistical measures for each basis set and various types of excited states (XLS)

■ AUTHOR INFORMATION

Corresponding Authors

Denis Jacquemin − *Nantes Université, CNRS, CEISAM UMR 6230, F-44000 Nantes, France; Institut Universitaire de France (IUF), F-75005 Paris, France;* orcid.org/0000-0002-4217-0708; Email: denis.jacquemin@univ-nantes.fr

Martial Boggio-Pasqua − *Laboratoire de Chimie et Physique Quantiques (UMR 5626), Université de Toulouse, CNRS, UPS, F-31062 Toulouse, France;* orcid.org/0000-0001-6684-5223; Email: martial.boggio@irsamc.ups-tlse.fr

Pierre-François Loos − *Laboratoire de Chimie et Physique Quantiques (UMR 5626), Université de Toulouse, CNRS, UPS, F-31062 Toulouse, France;* orcid.org/0000-0003-0598-7425; Email: loos@irsamc.ups-tlse.fr

Authors

Fábris Kossoski − *Laboratoire de Chimie et Physique Quantiques (UMR 5626), Université de Toulouse, CNRS, UPS, F-31062 Toulouse, France;* orcid.org/0000-0002-1627-7093

Franck Gam − *Nantes Université, CNRS, CEISAM UMR 6230, F-44000 Nantes, France*

Complete contact information is available at: https://pubs.acs.org/10.1021/acs.jctc.3c01080

Notes

The authors declare no competing financial interest.

■ ACKNOWLEDGMENTS

This work was performed using HPC resources from CALMIP (Toulouse) under allocation 2023-18005. F.G. and D.J. are indebted to the CCIPL/GliCID computational center installed in Nantes for a generous allocation of computational time. This project received funding from the European Research Council (ERC) under the European Union's Horizon 2020 Research and Innovation Programme (Grant Agreement 863481).

■ REFERENCES

(1) Khomskii, D. I. *Transition Metal Compounds*; Cambridge University Press, 2014.

(2) Trautwein, A. *Bioinorganic Chemistry: Transition Metals in Biology and Their Coordination Chemistry*; Wiley-VCH, 1997.

(3) Askerka, M.; Brudvig, G. W.; Batista, V. S. The Osub2/sub-Evolving Complex of Photosystem II: Recent Insights from Quantum Mechanics/Molecular Mechanics (QM/MM), Extended X-ray Absorption Fine Structure (EXAFS), and Femtosecond X-ray Crystallography Data. *Acc. Chem. Res.* **2017**, *50*, 41−48.

(4) Ebert, H. Magneto-optical effects in transition metal systems. *Rep. Prog. Phys.* **1996**, *59*, 1665−1735.

(5) van Oudenaarden, A.; Devoret, M. H.; Nazarov, Y. V.; Mooij, J. E. Magneto-electric Aharonov−Bohm effect in metal rings. *Nature* **1998**, *391*, 768−770.

(6) Gerhard, L.; Yamada, T. K.; Balashov, T.; Takács, A. F.; Wesselink, R. J. H.; Däne, M.; Fechner, M.; Ostanin, S.; Ernst, A.; Mertig, I.; Wulfhekel, W. Magnetoelectric coupling at metal surfaces. *Nat. Nanotechnol.* **2010**, *5*, 792−797.

(7) Melius, C. F. On the role of d electrons in chemisorption and catalysis on transition metal surfaces. *Chem. Phys. Lett.* **1976**, *39*, 287−290.

(8) Bolm, C.; Palazzi, C.; Beckmann, O. Metal-Catalyzed Baeyer-Villiger Reactions. In *Transition Metals for Organic Synthesis*, 2nd ed.; Beller, M., Bolm, C., Eds.; Wiley-VCH, 2004; Vol. 2, pp 267−274.

(9) Ma, C.; Fang, P.; Liu, D.; Jiao, K.-J.; Gao, P.-S.; Qiu, H.; Mei, T.-S. Transition metal-catalyzed organic reactions in undivided electrochemical cells. *Chem. Sci.* **2021**, *12*, 12866−12873.

(10) García-Melchor, M.; Braga, A. A. C.; Lledós, A.; Ujaque, G.; Maseras, F. Computational Perspective on Pd-Catalyzed C−C Cross-Coupling Reaction Mechanisms. *Acc. Chem. Res.* **2013**, *46*, 2626−2634.

(11) Guest, D.; Menezes da Silva, V. H.; de Lima Batista, A. P.; Roe, S. M.; Braga, A. A. C.; Navarro, O. (N-Heterocyclic Carbene)-Palladate Complexes in Anionic Mizoroki−Heck Coupling Cycles: A Combined Experimental and Computational Study. *Organometallics* **2015**, *34*, 2463−2470.

(12) Sperger, T.; Sanhueza, I. A.; Kalvet, I.; Schoenebeck, F. Computational Studies of Synthetically Relevant Homogeneous Organometallic Catalysis Involving Ni, Pd, Ir, and Rh: An Overview of Commonly Employed DFT Methods and Mechanistic Insights. *Chem. Rev.* **2015**, *115*, 9532−9586.

(13) Bernardi, F.; De, S.; Olivucci, M.; Robb, M. A. The Mechanism of Ground-State-Forbidden Photochemical Pericyclic Reactions: Evidence for Real Conical Intersections. *J. Am. Chem. Soc.* **1990**, *112*, 1737−1744.

(14) Klessinger, M.; Michl, J. *Excited States and Photochemistry of Organic Molecules*; VCH: New York, 1995.
(15) Robb, M. A.; Garavelli, M.; Olivucci, M.; Bernardi, F. A Computational Strategy for Organic Photochemistry. *Rev. Comput. Chem.* **2000**, *15*, 87−146.
(16) Delgado, J. L.; Bouit, P.-A.; Filippone, S.; Herranz, M.; Martín, N. Organic Photovoltaics: A Chemical Approach. *Chem. Commun.* **2010**, *46*, 4853.
(17) Olivucci, M. *Computational Photochemistry*; Elsevier Science: Amsterdam, 2010.
(18) Twilton, J.; Le, C.; Zhang, P.; Shaw, M. H.; Evans, R. W.; MacMillan, D. W. C. The merger of transition metal and photocatalysis. *Nat. Rev. Chem.* **2017**, *1*, 0052.
(19) Geneaux, R.; Marroux, H. J. B.; Guggenmos, A.; Neumark, D. M.; Leone, S. R. Transient absorption spectroscopy using high harmonic generation: a review of ultrafast X-ray dynamics in molecules and solids. *Philos. Trans. R. Soc. A* **2019**, *377*, 20170463.
(20) Haglund, R. F., Jr. Time and Space-Resolved Spectroscopy. In *Laser Ablation and Its Applications*; Phipps, C., Ed.; Springer, 2007; pp 185−213.
(21) Bokarev, S. I.; Kühn, O. Theoretical X-ray spectroscopy of transition metal compounds. *Wiley Interdiscip. Rev.: Comput. Mol. Sci.* **2020**, *10*, No. e1433.
(22) Harrison, J. F. Electronic Structure of Diatomic Molecules Composed of a First-Row Transition Metal and Main-Group Element (HF). *Chem. Rev.* **2000**, *100*, 679−716.
(23) Harvey, J. N. On the accuracy of density functional theory in transition metal chemistry. *Annu. Sect. C: Phys. Chem.* **2006**, *102*, 203.
(24) Zhao, Y.; Truhlar, D. G. Comparative assessment of density functional methods for 3d transition-metal chemistry. *J. Chem. Phys.* **2006**, *124*, 224105.
(25) Sperger, T.; Sanhueza, I. A.; Schoenebeck, F. Computation and Experiment: A Powerful Combination to Understand and Predict Reactivities. *Acc. Chem. Res.* **2016**, *49*, 1311−1319.
(26) Santoro, S.; Kalek, M.; Huang, G.; Himo, F. Elucidation of Mechanisms and Selectivities of Metal-Catalyzed Reactions using Quantum Chemical Methodology. *Acc. Chem. Res.* **2016**, *49*, 1006−1018.
(27) Friesner, R. A.; Jerome, S. V. Localized orbital corrections for density functional calculations on transition metal containing systems. *Coord. Chem. Rev.* **2017**, *344*, 205−213.
(28) Hait, D.; Tubman, N. M.; Levine, D. S.; Whaley, K. B.; Head-Gordon, M. What Levels of Coupled Cluster Theory Are Appropriate for Transition Metal Systems? A Study Using Near-Exact Quantum Chemical Values for 3d Transition Metal Binary Compounds. *J. Chem. Theory Comput.* **2019**, *15*, 5370−5385.
(29) Roos, B. O.; Andersson, K.; Fülscher, M. P.; Malmqvist, P.-Å.; Serrano-Andrés, L.; Pierloot, K.; Merchán, M. Multiconfigurational Perturbation Theory: Applications In Electronic Spectroscopy. *Adv. Chem. Phys.* **1996**, *93*, 219−331.
(30) Piecuch, P.; Kowalski, K.; Pimienta, I. S. O.; Mcguire, M. J. Recent advances in electronic structure theory: Method of moments of coupled-cluster equations and renormalized coupled-cluster approaches. *Int. Rev. Phys. Chem.* **2002**, *21*, 527−655.
(31) Dreuw, A.; Head-Gordon, M. Single-Reference Ab Initio Methods for the Calculation of Excited States of Large Molecules. *Chem. Rev.* **2005**, *105*, 4009−4037.
(32) Krylov, A. I. Spin-Flip Equation-of-Motion Coupled-Cluster Electronic Structure Method for a Description of Excited States, Bond Breaking, Diradicals, and Triradicals. *Acc. Chem. Res.* **2006**, *39*, 83−91.
(33) Sneskov, K.; Christiansen, O. Excited State Coupled Cluster Methods. *Wiley Interdiscip. Rev.: Comput. Mol. Sci.* **2012**, *2*, 566−584.
(34) González, L.; Escudero, D.; Serrano-Andrès, L. Progress and Challenges in the Calculation of Electronic Excited States. *ChemPhysChem* **2012**, *13*, 28−51.
(35) Laurent, A. D.; Jacquemin, D. TD-DFT Benchmarks: A Review. *Int. J. Quantum Chem.* **2013**, *113*, 2019−2039.
(36) Adamo, C.; Jacquemin, D. The Calculations of Excited-State Properties with Time-Dependent Density Functional Theory. *Chem. Soc. Rev.* **2013**, *42*, 845−856.
(37) Ghosh, S.; Verma, P.; Cramer, C. J.; Gagliardi, L.; Truhlar, D. G. Combining Wave Function Methods with Density Functional Theory for Excited States. *Chem. Rev.* **2018**, *118*, 7249−7292.
(38) Blase, X.; Duchemin, I.; Jacquemin, D.; Loos, P.-F. The Bethe-Salpeter Equation Formalism: From Physics to Chemistry. *J. Phys. Chem. Lett.* **2020**, *11*, 7371−7382.
(39) Loos, P. F.; Pradines, B.; Scemama, A.; Giner, E.; Toulouse, J. A Density-Based Basis-Set Incompleteness Correction for GW Methods. *J. Chem. Theory Comput.* **2020**, *16*, 1018−1028.
(40) Helgaker, T.; Jørgensen, P.; Olsen, J. *Molecular Electronic-Structure Theory*; John Wiley & Sons, 2013.
(41) Khedkar, A.; Roemelt, M. Modern multireference methods and their application in transition metal chemistry. *Phys. Chem. Chem. Phys.* **2021**, *23*, 17097−17112.
(42) Buendía, E.; Gálvez, F.; Maldonado, P.; Sarsa, A. Quantum Monte Carlo ionization potential and electron affinity for transition metal atoms. *Chem. Phys. Lett.* **2013**, *559*, 12−17.
(43) Aoto, Y. A.; de Lima Batista, A. P.; Köhn, A.; de Oliveira-Filho, A. G. S. How To Arrive at Accurate Benchmark Values for Transition Metal Compounds: Computation or Experiment? *J. Chem. Theory Comput.* **2017**, *13*, 5291−5316.
(44) Shee, J.; Rudshteyn, B.; Arthur, E. J.; Zhang, S.; Reichman, D. R.; Friesner, R. A. On Achieving High Accuracy in Quantum Chemical Calculations of 3*d* Transition Metal-Containing Systems: A Comparison of Auxiliary-Field Quantum Monte Carlo with Coupled Cluster, Density Functional Theory, and Experiment for Diatomic Molecules. *J. Chem. Theory Comput.* **2019**, *15*, 2346−2358.
(45) Wagner, L.; Mitáš, L. A quantum Monte Carlo study of electron correlation in transition metal oxygen molecules. *Chem. Phys. Lett.* **2003**, *370*, 412−417.
(46) Wagner, L. K.; Mitáš, L. Energetics and dipole moment of transition metal monoxides by quantum Monte Carlo. *J. Chem. Phys.* **2007**, *126*, 034105.
(47) Diedrich, C.; Lüchow, A.; Grimme, S. Performance of diffusion Monte Carlo for the first dissociation energies of transition metal carbonyls. *J. Chem. Phys.* **2005**, *122*, 021101.
(48) Caffarel, M.; Daudey, J.-P.; Heully, J.-L.; Ramírez-Solís, A. Towards accurate all-electron quantum Monte Carlo calculations of transition-metal systems: Spectroscopy of the copper atom. *J. Chem. Phys.* **2005**, *123*, No. 094102.
(49) Caffarel, M.; Giner, E.; Scemama, A.; Ramírez-Solís, A. Spin Density Distribution in Open-Shell Transition Metal Systems: A Comparative Post-Hartree-Fock, Density Functional Theory, and Quantum Monte Carlo Study of the $CuCl_2$ Molecule. *J. Chem. Theory Comput.* **2014**, *10*, 5286−5296.
(50) Doblhoff-Dier, K.; Meyer, J.; Hoggan, P. E.; Kroes, G.-J.; Wagner, L. K. Diffusion Monte Carlo for Accurate Dissociation Energies of 3d Transition Metal Containing Molecules. *J. Chem. Theory Comput.* **2016**, *12*, 2583−2597.
(51) Scemama, A.; Garniron, Y.; Caffarel, M.; Loos, P. F. Deterministic Construction Of Nodal Surfaces Within Quantum Monte Carlo: The Case Of FeS. *J. Chem. Theory Comput.* **2018**, *14*, 1395.
(52) Giner, E.; Tew, D. P.; Garniron, Y.; Alavi, A. Interplay between Electronic Correlation and Metal-Ligand Delocalization in the Spectroscopy of Transition Metal Compounds: Case Study on a Series of Planar Cu^{2+} Complexes. *J. Chem. Theory Comput.* **2018**, *14*, 6240−6252.
(53) Suo, B.; Shen, K.; Li, Z.; Liu, W. Performance of TD-DFT for Excited States of Open-Shell Transition Metal Compounds. *J. Phys. Chem. A* **2017**, *121*, 3929−3942.
(54) Nooijen, M.; Lotrich, V. Extended similarity transformed equation-of-motion coupled cluster theory (extended-STEOM-CC): Applications to doubly excited states and transition metal compounds. *J. Chem. Phys.* **2000**, *113*, 494−507.

https://doi.org/10.1021/acs.jctc.3c01080
J. Chem. Theory Comput. 2023, 19, 8782−8800

(55) Körbel, S.; Boulanger, P.; Duchemin, I.; Blase, X.; Marques, M. A. L.; Botti, S. Benchmark Many-Body GW and Bethe-Salpeter Calculations for Small Transition Metal Molecules. *J. Chem. Theory Comput.* **2014**, *10*, 3934−3943.
(56) Wang, X.-Y.; Avendaño, C.; Dunbar, K. R. Molecular magnetic materials based on 4d and 5d transition metals. *Chem. Soc. Rev.* **2011**, *40*, 3213−3238.
(57) Véril, M.; Scemama, A.; Caffarel, M.; Lipparini, F.; Boggio-Pasqua, M.; Jacquemin, D.; Loos, P.-F. QUESTDB: A database of highly accurate excitation energies for the electronic structure community. *Wiley Interdiscip. Rev.: Comput. Mol. Sci.* **2021**, *11*, e1517.
(58) Szabo, A.; Ostlund, N. S. *Modern Quantum Chemistry*; McGraw-Hill: New York, 1989.
(59) Andersson, K.; Malmqvist, P. A.; Roos, B. O.; Sadlej, A. J.; Wolinski, K. Second-Order Perturbation Theory With a CASSCF Reference Function. *J. Phys. Chem.* **1990**, *94*, 5483−5488.
(60) Andersson, K.; Malmqvist, P.-A.; Roos, B. O. Second-Order Perturbation Theory With a Complete Active Space Self-Consistent Field Reference Function. *J. Chem. Phys.* **1992**, *96*, 1218−1226.
(61) Roos, B. O.; Fülscher, M.; Malmqvist, P.-Å.; Merchán, M.; Serrano-Andrés, L. Theoretical Studies of the Electronic Spectra of Organic Molecules. In *Quantum Mechanical Electronic Structure Calculations with Chemical Accuracy*; Langhoff, S. R., Ed.; Springer: Dordrecht, The Netherlands, 1995; pp 357−438.
(62) Angeli, C.; Cimiraglia, R.; Malrieu, J.-P. N-Electron Valence State Perturbation Theory: A Fast Implementation of the Strongly Contracted Variant. *Chem. Phys. Lett.* **2001**, *350*, 297−305.
(63) Angeli, C.; Cimiraglia, R.; Evangelisti, S.; Leininger, T.; Malrieu, J.-P. Introduction of *n*-Electron Valence States for Multireference Perturbation Theory. *J. Chem. Phys.* **2001**, *114*, 10252−10264.
(64) Angeli, C.; Cimiraglia, R.; Malrieu, J.-P. *N* -Electron Valence State Perturbation Theory: A Spinless Formulation and an Efficient Implementation of the Strongly Contracted and of the Partially Contracted Variants. *J. Chem. Phys.* **2002**, *117*, 9138−9153.
(65) Angeli, C.; Bories, B.; Cavallini, A.; Cimiraglia, R. Third-order multireference perturbation theory: The n-electron valence state perturbation-theory approach. *J. Chem. Phys.* **2006**, *124*, 054108.
(66) Čížek, J. On the Correlation Problem in Atomic and Molecular Systems. Calculation of Wavefunction Components in Ursell-Type Expansion Using Quantum-Field Theoretical Methods. *J. Chem. Phys.* **1966**, *45*, 4256−4266.
(67) Čížek, J. On the Use of the Cluster Expansion and the Technique of Diagrams in Calculations of Correlation Effects in Atoms and Molecules. *Adv. Chem. Phys.* **1969**, *14*, 35−89.
(68) Paldus, J. Coupled Cluster Theory. In *Methods in Computational Molecular Physics*; Wilson, S., Diercksen, G. H. F., Eds.; Springer: Boston, MA, 1992; pp 99−194.
(69) Crawford, T. D.; Schaefer, H. F. An Introduction to Coupled Cluster Theory for Computational Chemists. *Rev. Comput. Chem.* **2000**, *14*, 33−136.
(70) Bartlett, R. J.; Musiał, M. Coupled-Cluster Theory in Quantum Chemistry. *Rev. Mod. Phys.* **2007**, *79*, 291−352.
(71) Shavitt, I.; Bartlett, R. J. *Many-Body Methods in Chemistry and Physics: MBPT and Coupled-Cluster Theory*; Cambridge Molecular Science; Cambridge University Press: Cambridge, U.K., 2009.
(72) Purvis, G. P., III; Bartlett, R. J. A Full Coupled-Cluster Singles and Doubles Model: The Inclusion of Disconnected Triples. *J. Chem. Phys.* **1982**, *76*, 1910−1918.
(73) Scuseria, G. E.; Scheiner, A. C.; Lee, T. J.; Rice, J. E.; Schaefer, H. F. The closed-shell coupled cluster single and double excitation (CCSD) model for the description of electron correlation. A comparison with configuration interaction (CISD) results. *J. Chem. Phys.* **1987**, *86*, 2881−2890.
(74) Koch, H.; Jensen, H. J. A.; Jørgensen, P.; Helgaker, T. Excitation Energies from the Coupled Cluster Singles and Doubles Linear Response Function (CCSDLR). Applications to Be, CH^+, CO, and H_2O. *J. Chem. Phys.* **1990**, *93*, 3345−3350.
(75) Stanton, J. F.; Bartlett, R. J. The equation of motion coupled-cluster method. A systematic biorthogonal approach to molecular excitation energies, transition probabilities, and excited state properties. *J. Chem. Phys.* **1993**, *98*, 7029−7039.
(76) Stanton, J. F. Many-body methods for excited state potential energy surfaces. I. General theory of energy gradients for the equation-of-motion coupled-cluster method. *J. Chem. Phys.* **1993**, *99*, 8840−8847.
(77) Noga, J.; Bartlett, R. J. The Full CCSDT Model for Molecular Electronic Structure. *J. Chem. Phys.* **1987**, *86*, 7041−7050.
(78) Scuseria, G. E.; Schaefer, H. F. A new implementation of the full CCSDT model for molecular electronic structure. *Chem. Phys. Lett.* **1988**, *152*, 382−386.
(79) Watts, J. D.; Bartlett, R. J. The inclusion of connected triple excitations in the equation-of-motion coupled-cluster method. *J. Chem. Phys.* **1994**, *101*, 3073−3078.
(80) Kucharski, S. A.; Włoch, M.; Musiał, M.; Bartlett, R. J. Coupled-cluster theory for excited electronic states: The full equation-of-motion coupled-cluster single, double, and triple excitation method. *J. Chem. Phys.* **2001**, *115*, 8263−8266.
(81) Kucharski, S. A.; Bartlett, R. J. Recursive Intermediate Factorization and Complete Computational Linearization of the Coupled-Cluster Single, Double, Triple, and Quadruple Excitation Equations. *Theor. Chim. Acta* **1991**, *80*, 387−405.
(82) Kállay, M.; Surján, P. R. Higher excitations in coupled-cluster theory. *J. Chem. Phys.* **2001**, *115*, 2945−2954.
(83) Hirata, S. Higher-Order Equation-of-Motion Coupled-Cluster Methods. *J. Chem. Phys.* **2004**, *121*, 51−59.
(84) Kállay, M.; Gauss, J.; Szalay, P. G. Analytic first derivatives for general coupled-cluster and configuration interaction models. *J. Chem. Phys.* **2003**, *119*, 2991−3004.
(85) Kállay, M.; Gauss, J. Analytic second derivatives for general coupled-cluster and configuration-interaction models. *J. Chem. Phys.* **2004**, *120*, 6841−6848.
(86) Christiansen, O.; Koch, H.; Jørgensen, P. The Second-Order Approximate Coupled Cluster Singles and Doubles Model CC2. *Chem. Phys. Lett.* **1995**, *243*, 409−418.
(87) Hättig, C.; Weigend, F. CC2 Excitation Energy Calculations on Large Molecules Using the Resolution of the Identity Approximation. *J. Chem. Phys.* **2000**, *113*, 5154−5161.
(88) Christiansen, O.; Koch, H.; Jørgensen, P. Response Functions in the CC3 Iterative Triple Excitation Model. *J. Chem. Phys.* **1995**, *103*, 7429−7441.
(89) Koch, H.; Christiansen, O.; Jørgensen, P.; Olsen, J. Excitation Energies of BH, CH_2 and Ne in Full Configuration Interaction and the Hierarchy CCS, CC2, CCSD and CC3 of Coupled Cluster Models. *Chem. Phys. Lett.* **1995**, *244*, 75−82.
(90) Koch, H.; Christiansen, O.; Jørgensen, P.; Sanchez de Merás, A. M.; Helgaker, T. The CC3Model: An Iterative Coupled Cluster Approach Including Connected Triples. *J. Chem. Phys.* **1997**, *106*, 1808−1818.
(91) Hald, K.; Jørgensen, P.; Olsen, J.; Jaszuński, M. An analysis and implementation of a general coupled cluster approach to excitation energies with application to the B_2 molecule. *J. Chem. Phys.* **2001**, *115*, 671−679.
(92) Paul, A. C.; Myhre, R. H.; Koch, H. New and Efficient Implementation of CC3. *J. Chem. Theory Comput.* **2021**, *17*, 117−126.
(93) Kállay, M.; Gauss, J. Calculation of Excited-State Properties Using General Coupled-Cluster and Configuration-Interaction Models. *J. Chem. Phys.* **2004**, *121*, 9257−9269.
(94) Kállay, M.; Gauss, J. Approximate treatment of higher excitations in coupled-cluster theory. *J. Chem. Phys.* **2005**, *123*, 214105.
(95) Matthews, D. A.; Stanton, J. F. Non-orthogonal spin-adaptation of coupled cluster methods: A new implementation of methods including quadruple excitations. *J. Chem. Phys.* **2015**, *142*, 064108.
(96) Loos, P.-F.; Comin, M.; Blase, X.; Jacquemin, D. Reference Energies for Intramolecular Charge-Transfer Excitations. *J. Chem. Theory Comput.* **2021**, *17*, 3666−3686.

https://doi.org/10.1021/acs.jctc.3c01080
J. Chem. Theory Comput. 2023, 19, 8782−8800

(97) Loos, P.-F.; Romaniello, P. Static and dynamic Bethe−Salpeter equations in the T-matrix approximation. *J. Chem. Phys.* **2022**, *156*, 164101.
(98) Rowe, D. J. Equations-of-Motion Method and the Extended Shell Model. *Rev. Mod. Phys.* **1968**, *40*, 153−166.
(99) Emrich, K. An extension of the coupled cluster formalism to excited states (I). *Nucl. Phys. A* **1981**, *351*, 379−396.
(100) Sekino, H.; Bartlett, R. J. A linear response, coupled-cluster theory for excitation energy. *Int. J. Quantum Chem.* **1984**, *26*, 255−265.
(101) Geertsen, J.; Rittby, M.; Bartlett, R. J. The equation-of-motion coupled-cluster method: Excitation energies of Be and CO. *Chem. Phys. Lett.* **1989**, *164*, 57−62.
(102) Comeau, D. C.; Bartlett, R. J. The equation-of-motion coupled-cluster method. Applications to open- and closed-shell reference states. *Chem. Phys. Lett.* **1993**, *207*, 414−423.
(103) Monkhorst, H. J. Calculation of properties with the coupled-cluster method. *Int. J. Quantum Chem.* **1977**, *12*, 421−432.
(104) Dalgaard, E.; Monkhorst, H. J. Some aspects of the time-dependent coupled-cluster approach to dynamic response functions. *Phys. Rev. A* **1983**, *28*, 1217−1222.
(105) Koch, H.; Jørgensen, P. Coupled cluster response functions. *J. Chem. Phys.* **1990**, *93*, 3333−3344.
(106) Pople, J. A.; Head-Gordon, M.; Fox, D. J.; Raghavachari, K.; Curtiss, L. A. Gaussian-1 theory: A general procedure for prediction of molecular energies. *J. Chem. Phys.* **1989**, *90*, 5622−5629.
(107) Curtiss, L. A.; Raghavachari, K.; Trucks, G. W.; Pople, J. A. Gaussian-2 Theory for Molecular Energies of First- and Second-row Compounds. *J. Chem. Phys.* **1991**, *94*, 7221−7230.
(108) Curtiss, L. A.; Raghavachari, K.; Redfern, P. C.; Pople, J. A. Assessment of Gaussian-2 and Density Functional Theories for the Computation of Enthalpies of Formation. *J. Chem. Phys.* **1997**, *106*, 1063−1079.
(109) Curtiss, L. A.; Raghavachari, K.; Redfern, P. C.; Rassolov, V.; Pople, J. A. Gaussian-3 (G3) theory for molecules containing first and second-row atoms. *J. Chem. Phys.* **1998**, *109*, 7764−7776.
(110) Curtiss, L. A.; Redfern, P. C.; Raghavachari, K. Gaussian-4 theory. *J. Chem. Phys.* **2007**, *126*, 084108.
(111) Jurečka, P.; Šponer, J.; Černý, J.; Hobza, P. Benchmark database of accurate (MP2 and CCSD(T) complete basis set limit) interaction energies of small model complexes, DNA base pairs, and amino acid pairs. *Phys. Chem. Chem. Phys.* **2006**, *8*, 1985−1993.
(112) Řezáč, J.; Riley, K. E.; Hobza, P. S66: A Well-balanced Database of Benchmark Interaction Energies Relevant to Biomolecular Structures. *J. Chem. Theory Comput.* **2011**, *7*, 2427−2438. PMID: 21836824
(113) van Setten, M. J.; Caruso, F.; Sharifzadeh, S.; Ren, X.; Scheffler, M.; Liu, F.; Lischner, J.; Lin, L.; Deslippe, J. R.; Louie, S. G.; Yang, C.; Weigend, F.; Neaton, J. B.; Evers, F.; Rinke, P. *GW* 100: Benchmarking G_0W_0 for Molecular Systems. *J. Chem. Theory Comput.* **2015**, *11*, 5665−5687.
(114) Stuke, A.; Kunkel, C.; Golze, D.; Todorović, M.; Margraf, J. T.; Reuter, K.; Rinke, P.; Oberhofer, H. Atomic Structures and Orbital Energies of 61,489 Crystal-Forming Organic Molecules. *Sci. Data* **2020**, *7*, 58.
(115) Tajti, A.; Szalay, P. G.; Császár, A. G.; Kállay, M.; Gauss, J.; Valeev, E. F.; Flowers, B. A.; Vázquez, J.; Stanton, J. F. HEAT: High accuracy extrapolated ab initio thermochemistry. *J. Chem. Phys.* **2004**, *121*, 11599−11613.
(116) Bomble, Y. J.; Vázquez, J.; Kállay, M.; Michauk, C.; Szalay, P. G.; Császár, A. G.; Gauss, J.; Stanton, J. F. High-accuracy extrapolated ab initio thermochemistry. II. Minor improvements to the protocol and a vital simplification. *J. Chem. Phys.* **2006**, *125*, 064108.
(117) Harding, M. E.; Vazquez, J.; Ruscic, B.; Wilson, A. K.; Gauss, J.; Stanton, J. F. High-Accuracy Extrapolated ab Initio Thermochemistry. III. Additional Improvements and Overview. *J. Chem. Phys.* **2008**, *128*, 114111.
(118) Motta, M.; Ceperley, D. M.; Chan, G. K.-L.; Gomez, J. A.; Gull, E.; Guo, S.; Jiménez-Hoyos, C. A.; Lan, T. N.; Li, J.; Ma, F.; et al. Towards the solution of the many-electron problem in real materials: Equation of state of the hydrogen chain with state-of-the-art many-body methods. *Phys. Rev. X* **2017**, *7*, 031059.
(119) Williams, K. T.; Yao, Y.; Li, J.; Chen, L.; Shi, H.; Motta, M.; Niu, C.; Ray, U.; Guo, S.; Anderson, R. J.; et al. Direct comparison of many-body methods for realistic electronic Hamiltonians. *Phys. Rev. X* **2020**, *10*, 011041.
(120) Mardirossian, N.; Head-Gordon, M. Thirty years of density functional theory in computational chemistry: an overview and extensive assessment of 200 density functionals. *Mol. Phys.* **2017**, *115*, 2315−2372.
(121) Goerigk, L.; Grimme, S. A General Database for Main Group Thermochemistry, Kinetics, and Noncovalent Interactions — Assessment of Common and Reparameterized (meta-)GGA Density Functionals. *J. Chem. Theory Comput.* **2010**, *6*, 107−126.
(122) Goerigk, L.; Grimme, S. A thorough benchmark of density functional methods for general main group thermochemistry, kinetics, and noncovalent interactions. *Phys. Chem. Chem. Phys.* **2011**, *13*, 6670−6688.
(123) Goerigk, L.; Grimme, S. Efficient and Accurate Double-Hybrid-Meta-GGA Density Functionals—Evaluation with the Extended GMTKN30 Database for General Main Group Thermochemistry, Kinetics, and Noncovalent Interactions. *J. Chem. Theory Comput.* **2011**, *7*, 291−309.
(124) Goerigk, L.; Hansen, A.; Bauer, C.; Ehrlich, S.; Najibi, A.; Grimme, S. A look at the density functional theory zoo with the advanced GMTKN55 database for general main group thermochemistry, kinetics and noncovalent interactions. *Phys. Chem. Chem. Phys.* **2017**, *19*, 32184−32215.
(125) Schreiber, M.; Silva-Junior, M. R.; Sauer, S. P. A.; Thiel, W. Benchmarks for Electronically Excited States: CASPT2, CC2, CCSD and CC3. *J. Chem. Phys.* **2008**, *128*, 134110.
(126) Silva-Junior, M. R.; Schreiber, M.; Sauer, S. P. A.; Thiel, W. Benchmarks for Electronically Excited States: Time-Dependent Density Functional Theory and Density Functional Theory Based Multireference Configuration Interaction. *J. Chem. Phys.* **2008**, *129*, 104103.
(127) Silva-Junior, M. R.; Schreiber, M.; Sauer, S. P. A.; Thiel, W. Benchmarks of Electronically Excited States: Basis Set Effects on CASPT2 Results. *J. Chem. Phys.* **2010**, *133*, 174318.
(128) Silva-Junior, M. R.; Sauer, S. P.; Schreiber, M.; Thiel, W. Basis Set Effects on Coupled Cluster Benchmarks of Electronically Excited States: CC3, CCSDR(3) and CC2. *Mol. Phys.* **2010**, *108*, 453−465.
(129) Silva-Junior, M. R.; Schreiber, M.; Sauer, S. P. A.; Thiel, W. Benchmarks of Electronically Excited States: Basis Set Effecs Benchmarks of Electronically Excited States: Basis Set Effects on CASPT2 Results. *J. Chem. Phys.* **2010**, *133*, 174318.
(130) Leang, S. S.; Zahariev, F.; Gordon, M. S. Benchmarking the Performance of Time-Dependent Density Functional Methods. *J. Chem. Phys.* **2012**, *136*, 104101.
(131) Schwabe, T.; Goerigk, L. Time-Dependent Double-Hybrid Density Functionals with Spin-Component and Spin-Opposite Scaling. *J. Chem. Theory Comput.* **2017**, *13*, 4307−4323.
(132) Casanova-Páez, M.; Dardis, M. B.; Goerigk, L. ωB2PLYP and ωB2GPPLYP: The First Two Double-Hybrid Density Functionals with Long-Range Correction Optimized for Excitation Energies. *J. Chem. Theory Comput.* **2019**, *15*, 4735−4744.
(133) Casanova-Páez, M.; Goerigk, L. Assessing the Tamm−Dancoff approximation, singlet−singlet, and singlet-triplet excitations with the latest long-range corrected double-hybrid density functionals. *J. Chem. Phys.* **2020**, *153*, 064106.
(134) Furche, F.; Ahlrichs, R. Adiabatic Time-Dependent Density Functional Methods for Excited State Properties. *J. Chem. Phys.* **2002**, *117*, 7433.
(135) Send, R.; Kühn, M.; Furche, F. Assessing Excited State Methods by Adiabatic Excitation Energies. *J. Chem. Theory Comput.* **2011**, *7*, 2376−2386.
(136) Winter, N. O. C.; Graf, N. K.; Leutwyler, S.; Hättig, C. Benchmarks for 0−0 Transitions of Aromatic Organic Molecules:

DFT/B3LYP, ADC(2), CC2, SOS-CC2 and SCS-CC2 Compared to High-resolution Gas-Phase Data. *Phys. Chem. Chem. Phys.* **2013**, *15*, 6623−6630.
(137) Dierksen, M.; Grimme, S. A density functional calculation of the vibronic structure of electronic absorption spectra. *J. Chem. Phys.* **2004**, *120*, 3544−3554.
(138) Goerigk, L.; Grimme, S. Assessment of TD-DFT Methods and of Various Spin Scaled CIS_nD and CC2 Versions for the Treatment of Low-Lying Valence Excitations of Large Organic Dyes. *J. Chem. Phys.* **2010**, *132*, 184103.
(139) Jacquemin, D.; Planchat, A.; Adamo, C.; Mennucci, B. A TD-DFT Assessment of Functionals for Optical 0−0 Transitions in Solvated Dyes. *J. Chem. Theory Comput.* **2012**, *8*, 2359−2372.
(140) Jacquemin, D.; Duchemin, I.; Blase, X. 0−0 Energies Using Hybrid Schemes: Benchmarks of TD-DFT, CIS(D), ADC(2), CC2, and BSE/GW formalisms for 80 Real-Life Compounds. *J. Chem. Theory Comput.* **2015**, *11*, 5340−5359.
(141) Kozma, B.; Tajti, A.; Demoulin, B.; Izsak, R.; Nooijen, M.; Szalay, P. G. A New Benchmark Set for Excitation Energy of Charge Transfer States: Systematic Investigation of Coupled Cluster Type Methods. *J. Chem. Theory Comput.* **2020**, *16*, 4213−4225.
(142) Loos, P.-F.; Jacquemin, D. Evaluating 0−0 Energies with Theoretical Tools: a Short Review. *ChemPhotoChem.* **2019**, *3*, 684−696.
(143) Loos, P.-F.; Scemama, A.; Jacquemin, D. The Quest for Highly Accurate Excitation Energies: A Computational Perspective. *J. Phys. Chem. Lett.* **2020**, *11*, 2374−2383.
(144) Loos, P. F.; Scemama, A.; Blondel, A.; Garniron, Y.; Caffarel, M.; Jacquemin, D. A Mountaineering Strategy to Excited States: Highly-Accurate Reference Energies and Benchmarks. *J. Chem. Theory Comput.* **2018**, *14*, 4360.
(145) Loos, P.-F.; Boggio-Pasqua, M.; Scemama, A.; Caffarel, M.; Jacquemin, D. Reference Energies for Double Excitations. *J. Chem. Theory Comput.* **2019**, *15*, 1939−1956.
(146) Loos, P. F.; Lipparini, F.; Boggio-Pasqua, M.; Scemama, A.; Jacquemin, D. A Mountaineering Strategy to Excited States: Highly-Accurate Energies and Benchmarks for Medium Sized Molecules. *J. Chem. Theory Comput.* **2020**, *16*, 1711−1741.
(147) Loos, P.-F.; Matthews, D. A.; Lipparini, F.; Jacquemin, D. How accurate are EOM-CC4 vertical excitation energies? *J. Chem. Phys.* **2021**, *154*, 221103.
(148) Loos, P.-F.; Lipparini, F.; Matthews, D. A.; Blondel, A.; Jacquemin, D. A Mountaineering Strategy to Excited States: Revising Reference Values with EOM-CC4. *J. Chem. Theory Comput.* **2022**, *18*, 4418−4427.
(149) Loos, P.-F.; Scemama, A.; Boggio-Pasqua, M.; Jacquemin, D. Mountaineering Strategy to Excited States: Highly Accurate Energies and Benchmarks for Exotic Molecules and Radicals. *J. Chem. Theory Comput.* **2020**, *16*, 3720−3736.
(150) Loos, P.-F.; Jacquemin, D. A Mountaineering Strategy to Excited States: Highly Accurate Energies and Benchmarks for Bicyclic Systems. *J. Phys. Chem. A* **2021**, *125*, 10174−10188.
(151) Loos, P.-F.; Galland, N.; Jacquemin, D. Theoretical 0−0 Energies with Chemical Accuracy. *J. Phys. Chem. Lett.* **2018**, *9*, 4646−4651.
(152) Loos, P.-F.; Jacquemin, D. Chemically Accurate 0−0 Energies with not-so-Accurate Excited State Geometries. *J. Chem. Theory Comput.* **2019**, *15*, 2481−2491.
(153) Chrayteh, A.; Blondel, A.; Loos, P.-F.; Jacquemin, D. Mountaineering Strategy to Excited States: Highly Accurate Oscillator Strengths and Dipole Moments of Small Molecules. *J. Chem. Theory Comput.* **2021**, *17*, 416.
(154) Sarkar, R.; Boggio-Pasqua, M.; Loos, P. F.; Jacquemin, D. Benchmark of TD-DFT and Wavefunction Methods for Oscillator Strengths and Excited-State Dipoles. *J. Chem. Theory Comput.* **2021**, *17*, 1117−1132.
(155) Sarkar, R.; Loos, P.-F.; Boggio-Pasqua, M.; Jacquemin, D. Assessing the Performances of CASPT2 and NEVPT2 for Vertical Excitation Energies. *J. Chem. Theory Comput.* **2022**, *18*, 2418−2436.
(156) Damour, Y.; Quintero-Monsebaiz, R.; Caffarel, M.; Jacquemin, D.; Kossoski, F.; Scemama, A.; Loos, P.-F. Ground- and Excited-State Dipole Moments and Oscillator Strengths of Full Configuration Interaction Quality. *J. Chem. Theory Comput.* **2023**, *19*, 221−234.
(157) Hait, D.; Head-Gordon, M. Excited State Orbital Optimization via Minimizing the Square of the Gradient: General Approach and Application to Singly and Doubly Excited States via Density Functional Theory. *J. Chem. Theory Comput.* **2020**, *16*, 1699−1710.
(158) Hait, D.; Head-Gordon, M. Orbital Optimized Density Functional Theory for Electronic Excited States. *J. Phys. Chem. Lett.* **2021**, *12*, 4517−4529.
(159) Zhu, H.; Zhao, R.; Lu, Y.; Liu, M.; Zhang, J.; Gao, J. Leveling the Mountain Range of Excited-State Benchmarking through Multistate Density Functional Theory. *J. Phys. Chem. A* **2023**, *127*, 8473−8485.
(160) Liang, J.; Feng, X.; Hait, D.; Head-Gordon, M. Revisiting the Performance of Time-Dependent Density Functional Theory for Electronic Excitations: Assessment of 43 Popular and Recently Developed Functionals from Rungs One to Four. *J. Chem. Theory Comput.* **2022**, *18*, 3460−3473.
(161) Grotjahn, R.; Kaupp, M. Assessment of hybrid functionals for singlet and triplet excitations: Why do some local hybrid functionals perform so well for triplet excitation energies? *J. Chem. Phys.* **2021**, *155*, 124108.
(162) Casanova-Páez, M.; Dardis, M. B.; Goerigk, L. ωB2PLYP and ωB2GPPLYP: The First Two Double-Hybrid Density Functionals with Long-Range Correction Optimized for Excitation Energies. *J. Chem. Theory Comput.* **2019**, *15*, 4735−4744.
(163) Casanova-Páez, M.; Goerigk, L. Time-Dependent Long-Range-Corrected Double-Hybrid Density Functionals with Spin-Component and Spin-Opposite Scaling: A Comprehensive Analysis of Singlet−Singlet and Singlet−Triplet Excitation Energies. *J. Chem. Theory. Comput.* **2021**, *17*, 5165−5186.
(164) Mester, D.; Kállay, M. A Simple Range-Separated Double-Hybrid Density Functional Theory for Excited States. *J. Chem. Theory Comput.* **2021**, *17*, 927−942.
(165) Mester, D.; Kállay, M. Spin-Scaled Range-Separated Double-Hybrid Density Functional Theory for Excited States. *J. Chem. Theory Comput.* **2021**, *17*, 4211−4224.
(166) Dash, M.; Feldt, J.; Moroni, S.; Scemama, A.; Filippi, C. Excited States with Selected Configuration Interaction-Quantum Monte Carlo: Chemically Accurate Excitation Energies and Geometries. *J. Chem. Theory Comput.* **2019**, *15*, 4896−4906.
(167) Otis, L.; Craig, I. M.; Neuscamman, E. A hybrid approach to excited-state-specific variational Monte Carlo and doubly excited states. *J. Chem. Phys.* **2020**, *153*, 234105.
(168) Dash, M.; Moroni, S.; Filippi, C.; Scemama, A. Tailoring CIPSI Expansions for QMC Calculations of Electronic Excitations: The Case Study of Thiophene. *J. Chem. Theory Comput.* **2021**, *17*, 3426−3434.
(169) Shepard, S.; Panadés-Barrueta, R. L.; Moroni, S.; Scemama, A.; Filippi, C. Double Excitation Energies from Quantum Monte Carlo Using State-Specific Energy Optimization. *J. Chem. Theory Comput.* **2022**, *18*, 6722−6731.
(170) Otis, L.; Neuscamman, E. A promising intersection of excited-state-specific methods from quantum chemistry and quantum Monte Carlo. *Wiley Interdiscip. Rev.: Comput. Mol. Sci.* **2023**, *13*, e1659.
(171) Boggio-Pasqua, M.; Jacquemin, D.; Loos, P.-F. Benchmarking CASPT3 vertical excitation energies. *J. Chem. Phys.* **2022**, *157*, No. 014103.
(172) King, D. S.; Hermes, M. R.; Truhlar, D. G.; Gagliardi, L. Large-Scale Benchmarking of Multireference Vertical-Excitation Calculations via Automated Active-Space Selection. *J. Chem. Theory Comput.* **2022**, *18*, 6065−6076.
(173) Wang, M.; Fang, W.-H.; Li, C. Assessment of State-Averaged Driven Similarity Renormalization Group on Vertical Excitation

https://doi.org/10.1021/acs.jctc.3c01080
J. Chem. Theory Comput. 2023, 19, 8782−8800

Energies: Optimal Flow Parameters and Applications to Nucleobases. *J. Chem. Theory Comput.* **2023**, *19*, 122−136.
(174) Gould, T.; Hashimi, Z.; Kronik, L.; Dale, S. G. Single Excitation Energies Obtained from the Ensemble "HOMO−LUMO Gap": Exact Results and Approximations. *J. Phys. Chem. Lett.* **2022**, *13*, 2452−2458.
(175) Kossoski, F.; Loos, P.-F. State-Specific Configuration Interaction for Excited States. *J. Chem. Theory Comput.* **2023**, *19*, 2258−2269.
(176) Dombrowski, D. R.; Schulz, T.; Kleinschmidt, M.; Marian, C. M. R2022: A DFT/MRCI Ansatz with Improved Performance for Double Excitations. *J. Phys. Chem. A* **2023**, *127*, 2011−2025.
(177) Kossoski, F.; Loos, P.-F. Seniority and Hierarchy Configuration Interaction for Radicals and Excited States. *J. Chem. Theory Comput.* 2023. DOI: 10.1021/acs.jctc.3c00946.
(178) Matthews, D. A.; Cheng, L.; Harding, M. E.; Lipparini, F.; Stopkowicz, S.; Jagau, T.-C.; Szalay, P. G.; Gauss, J.; Stanton, J. F. Coupled-Cluster Techniques for Computational Chemistry: The CFOUR Program Package. *J. Chem. Phys.* **2020**, *152*, 214108.
(179) Frisch, M. J.; Trucks, G. W.; Schlegel, H. B.; Scuseria, G. E.; Robb, M. A.; Cheeseman, J. R.; Scalmani, G.; Barone, V.; Petersson, G. A.; Nakatsuji, H.; Li, X.; Caricato, M.; Marenich, A.; Bloino, J.; Janesko, B. G.; Gomperts, R.; Mennucci, B.; Hratchian, H. P.; Ortiz, J. V.; Izmaylov, A. F.; Sonnenberg, J. L.; Williams-Young, D.; Ding, F.; Lipparini, F.; Egidi, F.; Goings, J.; Peng, B.; Petrone, A.; Henderson, T.; Ranasinghe, D.; Zakrzewski, V. G.; Gao, J.; Rega, N.; Zheng, G.; Liang, W.; Hada, M.; Ehara, M.; Toyota, K.; Fukuda, R.; Hasegawa, J.; Ishida, M.; Nakajima, T.; Honda, Y.; Kitao, O.; Nakai, H.; Vreven, T.; Throssell, K.; Montgomery, J. A., Jr.; Peralta, J. E.; Ogliaro, F.; Bearpark, M.; Heyd, J. J.; Brothers, E. N.; Kudin, K. N.; Staroverov, V. N.; Keith, T. A.; Kobayashi, R.; Normand, J.; Raghavachari, K.; Rendell, A. P.; Burant, J. C.; Iyengar, S. S.; Tomasi, J.; Cossi, M.; Millam, J. M.; Klene, M.; Adamo, C.; Cammi, R.; Ochterski, J. W.; Martin, R. L.; Morokuma, K.; Farkas, O.; Foresman, J. B.; Fox, D. J. *Gaussian 16*, rev. C.01; Gaussian, Inc.: Wallingford, CT, 2016.
(180) Giner, E.; Scemama, A.; Caffarel, M. Using perturbatively selected configuration interaction in quantum Monte Carlo calculations. *Can. J. Chem.* **2013**, *91*, 879−885.
(181) Giner, E.; Scemama, A.; Caffarel, M. Fixed-node diffusion Monte Carlo potential energy curve of the fluorine molecule F2 using selected configuration interaction trial wavefunctions. *J. Chem. Phys.* **2015**, *142*, 044115.
(182) Liu, W.; Hoffmann, M. R. iCI: Iterative CI toward full CI. *J. Chem. Theory Comput.* **2016**, *12*, 1169−1178.
(183) Holmes, A. A.; Umrigar, C. J.; Sharma, S. Excited states using semistochastic heat-bath configuration interaction. *J. Chem. Phys.* **2017**, *147*, 164111.
(184) Mussard, B.; Sharma, S. One-Step Treatment of Spin−Orbit Coupling and Electron Correlation in Large Active Spaces. *J. Chem. Theory Comput.* **2018**, *14*, 154−165.
(185) Tubman, N. M.; Levine, D. S.; Hait, D.; Head-Gordon, M.; Whaley, K. B. An efficient deterministic perturbation theory for selected configuration interaction methods. *arXiv (Condensed Matter.Strongly Correlated Electrons)*, August 6, 2018, 1808.02049, ver. 1. https://arxiv.org/abs/1808.02049 (accessed 2023-09-29).
(186) Chien, A. D.; Holmes, A. A.; Otten, M.; Umrigar, C. J.; Sharma, S.; Zimmerman, P. M. Excited States of Methylene, Polyenes, and Ozone from Heat-Bath Configuration Interaction. *J. Phys. Chem. A* **2018**, *122*, 2714−2722.
(187) Tubman, N. M.; Freeman, C. D.; Levine, D. S.; Hait, D.; Head-Gordon, M.; Whaley, K. B. Modern Approaches to Exact Diagonalization and Selected Configuration Interaction with the Adaptive Sampling CI Method. *J. Chem. Theory Comput.* **2020**, *16*, 2139−2159.
(188) Loos, P.-F.; Damour, Y.; Scemama, A. The performance of CIPSI on the ground state electronic energy of benzene. *J. Chem. Phys.* **2020**, *153*, 176101.
(189) Yao, Y.; Giner, E.; Li, J.; Toulouse, J.; Umrigar, C. J. Almost exact energies for the Gaussian-2 set with the semistochastic heat-bath configuration interaction method. *J. Chem. Phys.* **2020**, *153*, 124117.
(190) Zhang, N.; Liu, W.; Hoffmann, M. R. Iterative Configuration Interaction with Selection. *J. Chem. Theory Comput.* **2020**, *16*, 2296−2316.
(191) Damour, Y.; Véril, M.; Kossoski, F.; Caffarel, M.; Jacquemin, D.; Scemama, A.; Loos, P.-F. Accurate Full Configuration Interaction Correlation Energy Estimates for Five- and Six-Membered Rings. *J. Chem. Phys.* **2021**, *155*, 134104.
(192) Yao, Y.; Umrigar, C. J. Orbital Optimization in Selected Configuration Interaction Methods. *J. Chem. Theory Comput.* **2021**, *17*, 4183−4194.
(193) Zhang, N.; Liu, W.; Hoffmann, M. R. Further Development of iCIPT2 for Strongly Correlated Electrons. *J. Chem. Theory Comput.* **2021**, *17*, 949−964.
(194) Larsson, H. R.; Zhai, H.; Umrigar, C. J.; Chan, G. K.-L. The Chromium Dimer: Closing a Chapter of Quantum Chemistry. *J. Am. Chem. Soc.* **2022**, *144*, 15932−15937.
(195) Coe, J. P.; Moreno Carrascosa, A.; Simmermacher, M.; Kirrander, A.; Paterson, M. J. Efficient Computation of Two-Electron Reduced Density Matrices via Selected Configuration Interaction. *J. Chem. Theory Comput.* **2022**, *18*, 6690−6699.
(196) Huron, B.; Malrieu, J. P.; Rancurel, P. Iterative perturbation calculations of ground and excited state energies from multiconfigurational zeroth-order wavefunctions. *J. Chem. Phys.* **1973**, *58*, 5745−5759.
(197) Garniron, Y.; Gasperich, K.; Applencourt, T.; Benali, A.; Ferté, A.; Paquier, J.; Pradines, B.; Assaraf, R.; Reinhardt, P.; Toulouse, J.; Barbaresco, P.; Renon, N.; David, G.; Malrieu, J. P.; Véril, M.; Caffarel, M.; Loos, P. F.; Giner, E.; Scemama, A. Quantum Package 2.0: a open-source determinant-driven suite of programs. *J. Chem. Theory Comput.* **2019**, *15*, 3591.
(198) Smith, D. G. A.; Burns, L. A.; Simmonett, A. C.; Parrish, R. M.; Schieber, M. C.; Galvelis, R.; Kraus, P.; Kruse, H.; Di Remigio, R.; Alenaizan, A.; James, A. M.; Lehtola, S.; Misiewicz, J. P.; Scheurer, M.; Shaw, R. A.; Schriber, J. B.; Xie, Y.; Glick, Z. L.; Sirianni, D. A.; O'Brien, J. S.; Waldrop, J. M.; Kumar, A.; Hohenstein, E. G.; Pritchard, B. P.; Brooks, B. R.; Schaefer, H. F., III; Sokolov, A. Y.; Patkowski, K.; DePrince, A. E., III; Bozkaya, U.; King, R. A.; Evangelista, F. A.; Turney, J. M.; Crawford, T. D.; Sherrill, C. D. PSI4 1.4: Open-source software for high-throughput quantum chemistry. *J. Chem. Phys.* **2020**, *152*, 184108.
(199) Kállay, M.; Nagy, P. R.; Mester, D.; Rolik, Z.; Samu, G.; Csontos, J.; Csóka, J.; Szabó, P. B.; Gyevi-Nagy, L.; Hégely, B.; Ladjánszki, I.; Szegedy, L.; Ladóczki, B.; Petrov, K.; Farkas, M.; Mezei, P. D.; Ganyecz, A. The MRCC program system: Accurate quantum chemistry from water to proteins. *J. Chem. Phys.* **2020**, *152*, 074107.
(200) Werner, H.-J.; Knowles, P. J.; Manby, F. R.; Black, J. A.; Doll, K.; Heßelmann, A.; Kats, D.; Köhn, A.; Korona, T.; Kreplin, D. A.; Ma, Q.; Miller, T. F.; Mitrushchenkov, A.; Peterson, K. A.; Polyak, I.; Rauhut, G.; Sibaev, M. The Molpro quantum chemistry package. *J. Chem. Phys.* **2020**, *152*, 144107.
(201) Ghigo, G.; Roos, B. O.; Malmqvist, P.-Å. A Modified Definition of the Zeroth-Order Hamiltonian in Multiconfigurational Perturbation Theory (CASPT2). *Chem. Phys. Lett.* **2004**, *396*, 142−149.
(202) Zobel, J. P.; Nogueira, J. J.; Gonzalez, L. The IPEA Dilemma in CASPT2. *Chem. Sci.* **2017**, *8*, 1482−1499.
(203) Roos, B. O.; Andersson, K. Multiconfigurational Perturbation Theory with Level Shift — the Cr_2 Potential Revisited. *Chem. Phys. Lett.* **1995**, *245*, 215−223.
(204) Roos, B. O.; Andersson, K.; Fülscher, M. P.; Serrano-Andrés, L.; Pierloot, K.; Merchán, M.; Molina, V. Applications of level shift corrected perturbation theory in electronic spectroscopy. *J. Mol. Struct.: THEOCHEM* **1996**, *388*, 257−276.
(205) Ram, R.; Bernath, P. Fourier Transform Emission Spectroscopy of ScH and ScD: The New Singlet Electronic States A^1,D^1,E^1, and F^1. *J. Mol. Spectrosc.* **1997**, *183*, 263−272.

(206) Tabet, J.; Adem, Z.; Taher, F. Ab initio investigation of ground and excited states of ScH molecule. *Spectrochim. Acta, Part A* **2021**, *256*, 119742.
(207) Chalek, C. L.; Gole, J. L. Chemiluminescence spectra of ScO and YO: Observation and analysis of the $A'^2\Delta-X^2\Sigma^+$ band system. *J. Chem. Phys.* **1976**, *65*, 2845−2859.
(208) Chalek, C. L.; Gole, J. L. Single collision chemiluminescence studies of scandium and yttrium oxidation with O_2, NO_2, N_2O and O_3. *Chem. Phys.* **1977**, *19*, 59−90.
(209) Jiang, T.; Chen, Y.; Bogdanov, N. A.; Wang, E.; Alavi, A.; Chen, J. A full configuration interaction quantum Monte Carlo study of ScO, TiO, and VO molecules. *J. Chem. Phys.* **2021**, *154*, 164302.
(210) Huber, K. P.; Herzberg, G. *Molecular Spectra and Molecular Structure: IV. Constants of Diatomic Molecules*; Springer: Boston, MA, 1979; pp 8−689.
(211) Lebeaultdorget, M.; Effantin, C.; Bernard, A.; Dincan, J.; Chevaleyre, J.; Shenyavskaya, E. Singlet States of ScF Below 23 000 cm^{-1}: $X^1\Sigma^+$, $A^1\Delta$, $B^1\Pi$, $C^1\Sigma^+$, $D^1\Pi$, and $E^1\Delta$. *J. Mol. Spectrosc.* **1994**, *163*, 276−283.
(212) Shenyavskaya, E.; Ross, A.; Topouzkhanian, A.; Wannous, G. Low-Lying Electronic States of the ScF Molecule: Energies of the a3, b3, and A1 States. *J. Mol. Spectrosc.* **1993**, *162*, 327−334.
(213) Langhoff, S. R.; Bauschlicher, C. W., Jr.; Partridge, H. Theoretical study of the scandium and yttrium halides. *J. Chem. Phys.* **1988**, *89*, 396−407.
(214) Romeu, J. G. F.; Belinassi, A. R.; Ornellas, F. R. Transition moments, radiative transition probabilities, and radiative lifetimes for the band systems $A^2\Pi-X^2\Sigma^+$, $B^2\Sigma^+-X^2\Sigma^+$, and $A^2\Pi-A'^2\Delta$ of scandium monosulfide, ScS. *J. Quant. Spectrosc. Radiat. Transfer* **2018**, *211*, 44−49.
(215) Gengler, J.; Chen, J.; Steimle, T.; Ram, R.; Bernath, P. A study of the $A^2\Pi-X^2\Sigma^+$ and $B^2\Sigma^+-X^2\Sigma^+$ band systems of scandium monosulfide, ScS, using Fourier transform emission spectroscopy and laser excitation spectroscopy. *J. Mol. Spectrosc.* **2006**, *237*, 36−45.
(216) Brabaharan, K.; Coxon, J.; Yamashita, A. Vibrational analysis of the titanium nitride emission spectrum. The A2 - X2 and B2 - A2 systems. *Spectrochim. Acta, Part A* **1985**, *41*, 847−850.
(217) Harrison, J. F. Electronic Structure of the Transition Metal Nitrides TiN, VN, and CrN. *J. Phys. Chem.* **1996**, *100*, 3513−3519.
(218) Xu, M.-S.; Yang, C.-L.; Wang, M.-S.; Ma, X.-G. Theoretical study on the low-lying excited electronic states and laser cooling feasibility of CuH molecule. *Spectrochim. Acta, Part A* **2019**, *212*, 55−60.
(219) Calvi, R. M.; Andrews, D. H.; Lineberger, W. C. Negative ion photoelectron spectroscopy of copper hydrides. *Chem. Phys. Lett.* **2007**, *442*, 12−16.
(220) Ahmed, F.; Barrow, R. F.; Chojnicki, A. H.; Dufour, C.; Schamps, J. Electronic states of the CuF molecule. I. Analysis of rotational structure. *J. Phys. B: At. Mol. Opt. Phys.* **1982**, *15*, 3801.
(221) Guichemerre, M.; Chambaud, G.; Stoll, H. Electronic structure and spectroscopy of monohalides of metals of group I-B. *Chem. Phys.* **2002**, *280*, 71−102.
(222) Delaval, J.; Lefebvre, Y.; Bocquet, H.; Bernage, P.; Niay, P. Radiative lifetimes of the low-lying electronic states of CuF and CuCl: Identification of the excited states of CuCl. *Chem. Phys.* **1987**, *111*, 129−136.
(223) Kim, J. H.; Li, X.; Wang, L.-S.; de Clercq, H. L.; Fancher, C. A.; Thomas, O. C.; Bowen, K. H. Vibrationally Resolved Photoelectron Spectroscopy of MgO- and ZnO- and the Low-Lying Electronic States of MgO, MgO-, and ZnO. *J. Phys. Chem. A* **2001**, *105*, 5709−5718.
(224) Sakellaris, C. N.; Papakondylis, A.; Mavridis, A. Ab initio Study of the Electronic Structure of Zinc Oxide and its Ions, ZnO(0, +/−). Ground and Excited States. *J. Phys. Chem. A* **2010**, *114*, 9333−9341.
(225) Moravec, V. D.; Klopcic, S. A.; Chatterjee, B.; Jarrold, C. C. The electronic structure of ZnO and ZnF determined by anion photoelectron spectroscopy. *Chem. Phys. Lett.* **2001**, *341*, 313−318.
(226) Papakondylis, A. Ab initio study of the ground and excited states of the zinc sulfide diatomic system, ZnS. *Chem. Phys. Lett.* **2011**, *512*, 44−48.
(227) Jamorski, C.; Dargelos, A.; Teichteil, C.; Daudey, J. P. Theoretical determination of spectral lines for the Zn atom and the ZnH molecule. *J. Chem. Phys.* **1994**, *100*, 917−925.
(228) Saue, T.; Bast, R.; Gomes, A. S. P.; Jensen, H. J. A.; Visscher, L.; Aucar, I. A.; Di Remigio, R.; Dyall, K. G.; Eliav, E.; Fasshauer, E.; Fleig, T.; Halbert, L.; Hedegård, E. D.; Helmich-Paris, B.; Iliaš, M.; Jacob, C. R.; Knecht, S.; Laerdahl, J. K.; Vidal, M. L.; Nayak, M. K.; Olejniczak, M.; Olsen, J. M. H.; Pernpointner, M.; Senjean, B.; Shee, A.; Sunaga, A.; van Stralen, J. N. P. The DIRAC code for relativistic molecular calculations. *J. Chem. Phys.* **2020**, *152*, 204104.

https://doi.org/10.1021/acs.jctc.3c01080
J. Chem. Theory Comput. 2023, 19, 8782−8800